Available online at www.sciencedirect.com
SCIENCE DIRECT®
Agricultural and Forest Meteorology 126 (2004) 271–295
AGRICULTURAL AND FOREST METEOROLOGY
www.elsevier.com/locate/agrformet

# Carbon exchange and venting anomalies in an upland deciduous forest in northern Wisconsin, USA

Bruce D. Cook[a,*], Kenneth J. Davis[b], Weiguo Wang[b], Ankur Desai[b], Bradford W. Berger[c], Ron M. Teclaw[d], Jonathan G. Martin[a], Paul V. Bolstad[a], Peter S. Bakwin[e], Chuixiang Yi[b], Warren Heilman[f]

[a]*Department of Forest Resources, University of Minnesota, 1530 North Cleveland Avenue, Saint Paul, MN 55108, USA*
[b]*Department of Meteorology, The Pennsylvania State University, 503 Walker Building, University Park, PA 16802-5013, USA*
[c]*Copper Mountain Community College, 6162 Rotary Way, PO Box 1398, Joshua Tree, CA 92252, USA*
[d]*USDA Forest Service, North Central Research Station, 5985 Highway K, Rhinelander, WI 54501, USA*
[e]*Climate Monitoring and Diagnostics Laboratory, National Oceanic and Atmospheric Administration, R/CMDL1, 325 Broadway, Boulder, CO 80305, USA*
[f]*USDA Forest Service, North Central Research Station, 1407 S. Harrison Road, Ste. 220, East Lansing, MI 48823, USA*

Accepted 17 June 2004

**Abstract**

Turbulent fluxes of carbon, water vapor, and temperature were continuously measured above an upland forest in north central Wisconsin during 1999 and 2000 using the eddy covariance method. Maple (*Acer saccharum*), basswood (*Tilia americana*), and green ash (*Fraxinus pennsylvanica*) species found in this forest also comprise a substantial portion of the landscape in the northern Great Lakes region and area, and it has been hypothesized that forests of this age (60–80 years) are responsible for net uptake of atmospheric $CO_2$ over North America. Mean $CO_2$, water vapor, and temperature profile measurements were used to improve flux estimates during periods of low turbulence, and were effective for friction velocities ($u_*$) >0.3 m $s^{-1}$. Unique observations at this site included nighttime and early morning venting anomalies that seemed to originate from a seemingly homogenous area within the forest. These elevated NEE measurements, some as high as 80 mol $m^{-2}$ $s^{-1}$, appeared in valid turbulent flux observations for hours at a time, and provided circumstantial evidence for preferential venting and/or existence of pooled $CO_2$ in low-lying areas. We observed that the forest was a moderate sink for atmospheric carbon, and cumulative NEE of $CO_2$ was estimated to be −334 g C $m^{-2}$ $year^{-1}$ during 2000. Sensitivity to low-turbulence flux corrections was very small (21 g C $m^{-2}$ $year^{-1}$), and discrepancies between annual estimates of NEE and NEP were similar to other sites. A normalized measure of ecosystem respiration, the free energy of activation, was presented and its seasonal variations were analyzed. Gross ecosystem production (GEP) was high (1165 g C $m^{-2}$ $year^{-1}$) and ecosystem respiration (ER) was low (817 g C $m^{-2}$ $year^{-1}$) in comparison to spatially integrated, landscape-scale observations from WLEF (914 and 1005 g C $m^{-2}$ $year^{-1}$, respectively), a 477 m tower located 22 km to the northeast [Glob. Change Biol. 9 (2003) 1278]. Forest transpiration was responsible for most of

* Corresponding author. Tel.: +1 612 624 9796; fax: +1 612 625 5212.
*E-mail address:* bcook@essc.psu.edu (B.D. Cook).

0168-1923/$ – see front matter 
doi:10.1016/j.agrformet.2004.06.008

the water released to the atmosphere. Stomata closed under intense sunlight and high vapor pressure deficits (VPD > 1.5 kPa). Effect of stomotal closure on annual $CO_2$ uptake was minimal due to adequate soil moisture and moderate VPD during the growing season.


*Keywords:* Eddy correlation; Deciduous forest; Carbon cycle; Nocturnal boundary layer; Evapotranspiration; Stomatal closure

## 1. Introduction

Rising concentrations of carbon dioxide ($CO_2$) in the atmosphere have received considerable attention from scientists and policy makers, because $CO_2$ is emitted to the atmosphere by anthropogenic activities and contributes to climate change (Houghton et al., 2001; Schlesinger, 1997). The terrestrial biosphere is a large and dynamic reservoir of carbon that can exchange with the atmosphere on short time scales (hours to decades); however, sources and sinks are not well defined (House et al., 2003; Ciais et al., 1995; Tans et al., 1990), and causes of spatial and temporal variability of the carbon balance of the terrestrial biosphere are not well understood (Houghton, 2003; Conway et al., 1994; Keeling et al., 1996). To enhance our understanding of the terrestrial carbon cycle, a global network of sites has been established to conduct continuous, long-term observations of carbon and water vapor exchange between terrestrial ecosystems and the atmosphere (Baldocchi et al., 2001).

Numerous studies have quantified carbon pools and flows in northern temperate and boreal forests stands, but few have encompassed regional scales (hundreds of $km^2$) on a continuous basis for multiple years. This is an objective of the Chequamegon Ecosystem–Atmosphere Study (ChEAS), currently being carried out in the Chequamegon-Nicolet National Forest of north central Wisconsin, using a network of eddy covariance measurements and biophysical observations (http://cheas.psu.edu/). A centerpiece of ChEAS is eddy flux measurements of $CO_2$ and $H_2O$ exchange from a 447 m tall TV transmitter tower (Davis et al., 2003; Berger et al., 2001), which is unique among the global network both because observations from its multiple levels integrate many different land cover and soil types, and because the tower is part of the National Oceanographic and Atmospheric Administration's tall tower $CO_2$ monitoring network (Bakwin et al., 1998). One goal of ChEAS is to measure stand-scale and component carbon fluxes within nearby representative forest stands, to analyze the relationships between these component and whole-stand fluxes, and develop and test methods to upscale $CO_2$ fluxes to landscape-scale observations from the tall tower. To this end we have established stand-scale observations at three sites near the tall tower: an upland deciduous forest (Willow Creek), an alder–willow–sedge wetland (Lost Creek), and an old-growth maple–hemlock forest (Sylvania Wilderness Area).

In this paper, we present observations of net ecosystem exchange of $CO_2$ (NEE) and evapotranspiration from the upland deciduous forest located at the Willow Creek study site, which is located 22 km from the tall tower. This forest is composed of broadleaf tree species that comprise a substantial portion of the landscape in the northern Great Lakes region and the area surrounding the tall tower. The stand is approximately 60–80 years old, and is typical of re-growth that may be responsible for some of the uptake of $CO_2$ in North America (Caspersen et al., 2000; Pacala et al., 2001). A 30 m tower was installed at this site and instrumented to measure $CO_2$ and $H_2O$ mixing ratio profiles, and fluxes of $CO_2$, latent heat, and sensible heat using the eddy covariance method. This paper describes methods that were used at each of the three stand-scale eddy covariance towers, and presents initial observations from the first 2 years of operation (1999 and 2000) at the Willow Creek upland hardwood site. Scaling up of stand-scale fluxes from this site and others in the region will be discussed in a future publication.

## 2. Materials and method

### 2.1. Site description and flux source area

Measurements were collected in an upland hardwood forest of the Chequamegon-Nicolet National Forest in northern Wisconsin (45.806°N, 90.080°W, elevation approximately 515 m). This 60–80-year-old

stand has a closed canopy approximately 24 m in height with a leaf area index (LAI) of 5.3 (unpublished data), and consists primarily of sugar maple (*Acer saccharum*), basswood (*Tilia americana*), and green ash (*Fraxinus pennsylvanica*). The understory is composed of sugar maple and ironwood (*Ostrya virginiana*) saplings, leatherwood (*Dirca palustris*), maidenhair (*Adiantum pedatum*) and bracken ferns (*Pteridium aquilinum*), and blue cohosh (*Caulophyllum thalictroides*).

The stand occupies about 260 ha, and is relatively homogeneous within 0.6 km of the tower, the approximate flux footprint, except for a minor drainageway (about 80 m wide) located about 0.3 km west of the observation tower (Fig. 1) which is characterized by red maple (*Acer rubrum*), black ash (*Fraxinus nigra*), and slippery elm (*Ulmus rubra*). Semi-analytical models (Massman, 1987) were used to estimate displacement height ($d$) and aerodynamic properties of the stand ($z_0$) based on LAI measurements and drag coefficients ($C_d$) observed during the leaf-on period. Flux footprint estimates (Horst and Weil, 1994) were calculated for an effective measurement height ($z_m$) of 13.2 m, a roughness length ($z_0$) of 2.3 m, and stability conditions (Monin-Obukov length, $L$) observed at $z_m$. During the growing season, model estimates suggested that 90% of the observed carbon flux emanated from within 0.4 and 0.6 km of the tower during daytime and nighttime, respectively, and source probability density functions peaked at distances of 0.025 and 0.035 km. Forested wetlands to the south impinge upon the nighttime footprint, but landscape features between 0.3 and 0.6 km were only responsible for 10% of the flux source.

Glacial features such as drumlins, moraines, poorly drained depressions, and outwash plains are typical

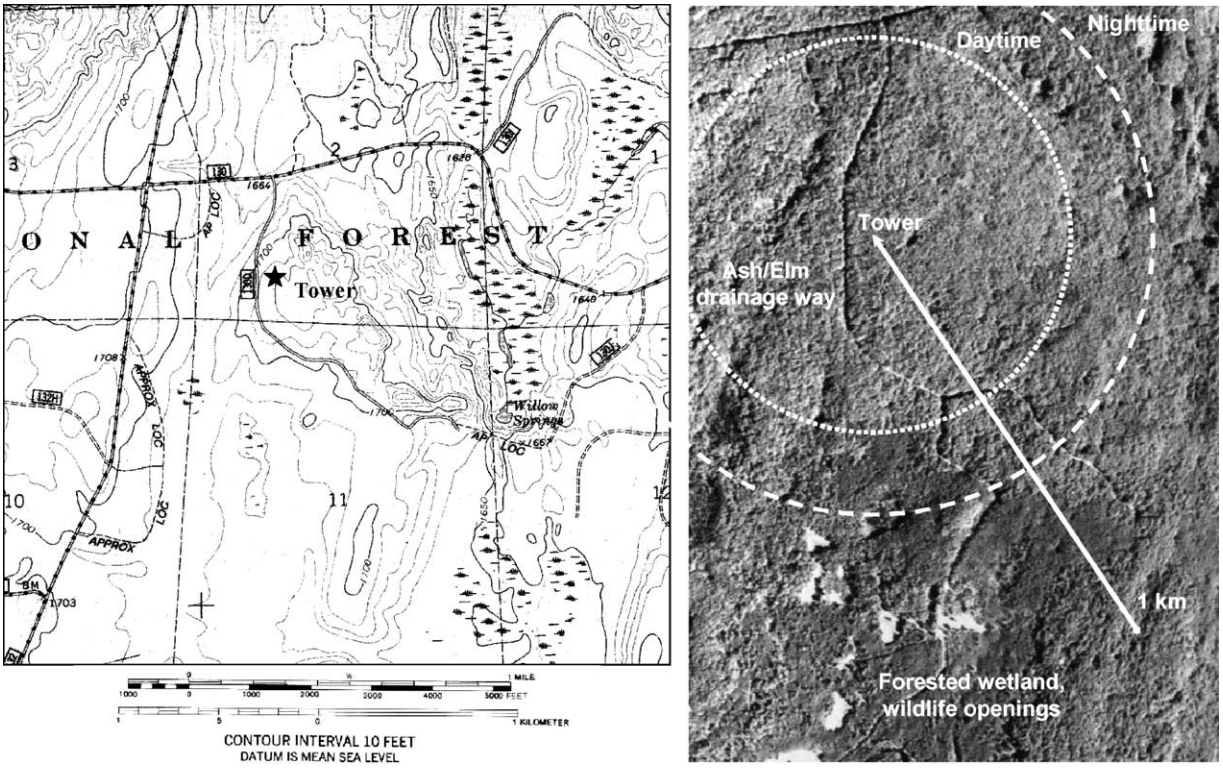


Fig. 1. (a) Local topography at the Willow Creek flux tower site (US Geological Survey, Pike Lake SE, Wisconsin, scale 1:24 000, series V861, sheet 1, US Government Printing Office, 1997); (b) estimated daytime and nighttime tower footprint ($u_* > 0.3$ m s$^{-1}$) shown on a multi-spectral image of vegetation (ATLAS aircraft, 1998; bands 6, 7, 4). An arrow is used to indicate the wind vector associated with the largest nighttime and early morning venting anomalies.

features of the regional landscape (Hole, 1976), and upland areas are generally characterized by slightly elevated ground moraines and southwest-trending drumlins. The terrain of the upland forest at Willow Creek is rolling to undulating, and elevation ranges from 490 to 530 m across low profile, oval-shaped ridges (Fig. 1). Slope at the tower base is about 1%, sloping downward towards the southwest.

Sandy loam soils at this site (about 54% sand, 33% silt, and 13% clay in the upper 30 cm) have developed from acidic, reddish, unsorted, coarse glacial till with 10–40% rock fragments. Soils have been subjected to mixing by windthrows, burrowing animals and earthworm activity, and frost action. Mottling and saturated soils were observed between 50 and 100 cm below the surface at different times during the year in these somewhat poorly drained soils. Total carbon and nitrogen in the litter layer and underlying mineral soil (0–30 cm) was about 10.7 and 0.74 kg $m^{-2}$, respectively. Soil water holding capacity was high at this site, and soil water contents were consistently high throughout this study. Sugar maple has the highest probability of becoming the dominant, late-successional tree species during forest regeneration on upland sites in northern Wisconsin that are characterized by high soil nutrient and water availabilities, such as Willow Creek (Walters and Reich, 1997; Curtis, 1959).

Land surveys conducted between 1857 and 1886 (Schulte and Mladenoff, 2001) indicate that pre-European settlement vegetation consisted primarily of hemlock (*Tsuga canadensis*), birch (*Betula* spp.), sugar maple (*A. saccharum*), and basswood (*T. americana*; unpublished data, Pre-European Settlement Vegetation Database of Wisconsin, Department of Forest Ecology and Management, University of Wisconsin-Madison, 2000). Diameters of ''witness'' trees, trees sampled in early land surveys, ranged from about 25 to 35 cm. The forests in this region were harvested extensively by the early 1900s, and it is likely that trees growing on this site were harvested at least twice since these early land surveys.

### 2.2. Eddy covariance measurements

A 30 m triangular tower (Rohn, Peoria, IL, model 45G) was instrumented at 29.6 m above the soil surface, about 5 m above the forest canopy, for carbon and energy flux measurements using the eddy covariance method. Power was supplied by a propane generator located 0.5 km north of the tower, an infrequent wind direction at the edge of the flux footprint, which charged a battery bank twice daily for 30–60 min. A three-dimensional sonic anemometer (Campbell Scientific Instruments, Logan, UT, model CSAT-3) was used to measure wind speeds and virtual temperature, and an infrared gas analyzer (Li-Cor, Lincoln, NE, model LI-6262) was used to measure fluctuations of $CO_2$ and $H_2O$ vapor mixing ratios. Measurements were collected at a frequency of 10 Hz, and the gas analyzer was calibrated with low frequency, high precision $CO_2$ and humidity measurements of the ambient air, as described by Berger et al. (2001). Low frequency $CO_2$ profile measurements were measured with a similar gas analyzer (see $CO_2$ profile measurements below), and humidity was measured using a chilled mirror hygrometer (EdgeTech, Milford, MA, model 200 DewTrak) and a relative humidity probe (Campbell Scientific Instruments, model CS500). The anemometer and air sample inlet were attached to the end of a 2 m boom pointed in the predominant wind direction (west). Air was drawn through a Teflon filter (1 μm pore size) and 2.9 m of Teflon PFA tubing (3.96 mm i.d.) before passing through the gas analyzer and diaphragm pump (Brailsford & Co., Rye, NY, model TD-4X2). Measurements were made in absolute mode by maintaining a constant flow of $CO_2$/$H_2O$-free $N_2$ gas through the reference cell at about 0.01 L $min^{-1}$. Sample flow rates were about 3 L $min^{-1}$, and average lag times observed for $CO_2$ and $H_2O$ were 1.3 and 2.1 s, respectively. An average Reynolds number of 650 indicated laminar flow within the sample tube, but analysis of $CO_2$ and $H_2O$ spectra (see Berger et al. (2001)) showed no degradation at frequencies less than 1 and 0.8 Hz, respectively (see results section). 'White' noise was observed in both the spectra at frequencies greater than 1 Hz.

### 2.3. $CO_2$ vertical profile measurements

Mixing ratios of $CO_2$ were measured at 0.6, 1.5, 3.0, 7.6, 13.7, 21.3, and 29.6 m above the soil surface using an infrared gas analyzer (Li-Cor, Lincoln, NE, model LI-6251). Zhao et al. (1997) and Bakwin et al. (1995) describe a similar system for obtaining high

precision $CO_2$ measurements at unattended sites, where precision of $<0.2$ ppm $CO_2$ is desired. Solenoid valves (Neumatics, Inc., Highland, MI, model L01) were used to control flow from each of the levels and each of three working gas standards (approximately 340, 440, and 550 ppm $CO_2$ in dry air) through analyzer sample cell. Mixing ratios of $CO_2$ in working gas standards (accurate to about $\pm 0.2$ ppm $CO_2$) were determined with an infrared gas analyzer that was calibrated with $CO_2$ standards (approximately 340 and 550 ppm, accurate to $\pm 0.01$ ppm) prepared by the Climate Monitoring and Diagnostics Laboratory of the National Oceanic and Atmospheric Administration (Kitzis and Zhao, 1999).

Measurements were made in differential mode by maintaining a constant flow ($\sim 0.01$ L min$^{-1}$) of compressed dry air containing approximately 440 ppm $CO_2$ through the reference cell of the analyzer. A backpressure regulator (Porter Instrument, Hatfield, IA, model 9000) was used to equalize pressure in the sample and reference cells. Samples of air from the tower profile were drawn through a Teflon filter (1 μm pore size) and variable lengths of Dekabon tubing (Saint-Gobain Performance Plastic, Wayne, NJ, model 1300, 5.5 mm i.d.) to the analyzer at the tower base. Air entering the sample cell was dried in a Nafion drier (Permapure, Toms River, NJ, model MD-050-72P using a countercurrent of $N_2$ gas) followed by a chemical desiccant ($Mg(ClO_4)_2$). Air was drawn continuously through each tube, and each height was sampled for 3 min every 21 min. Two minutes were required to flush the system (i.e., solenoid manifold, Nafion and chemical desiccant tubes, Li-Cor sample cell, and associated plumbing) at a flow rate of 0.1 L min$^{-1}$, and measurements were collected and averaged during the following minute. For each height, a cubic spline function (Research Systems, Inc., 1998) was used to interpolate 3 min data between actual measurements. Reference cell gas was passed through the sample cell every 42 min to obtain a ''zero'' value and a sequence of all three standards was measured every 3–4 h. Standard gas concentrations and measured output voltages were used to determine coefficients for a second order polynomial of the function suggested by the manufacturer (Li-Cor, 1996), and coefficients were interpolated using a cubic spline function to obtain calibration equations for each 3 min measurement.

### 2.4. Micrometeorological observations and data acquisition

Radiation and atmospheric pressure were measured at a frequency of 1 Hz with sensors mounted on the tower at 29.6 m. Four individual sensors were used for measuring incoming and reflected solar radiation, and incoming and emitted infrared radiation (Kipp & Zonan, Bohemia, NY, model CNR1); net radiation ($R_n$) was calculated by summing values from all four sensors. A quantum sensor (Li-Cor, Lincoln, NE, model LI190SZ) was used to measure incoming photosynthetically active radiation ($Q$). Ambient atmospheric pressure was measured with a barometer equipped with a silicon capacitive sensor (Vaisala, Helsinki, Finland, model PTB101B).

Air and soil temperature profiles, soil moisture and soil heat flux ($G_s$) were measured every 10 min. Platinum resistance temperature probes (R.M. Young, Traverse City, MI, model 41342; Campbell Scientific, Inc., Logan, UT, model CS500) and Cu–Cs thermocouples (type T) were positioned at 29.6, 24.4, 18.3, 12.2, 7.6, 1.0, 0.5, 0.2, 0.1, and 0.05 m above the soil surface to measure the air temperature, and atmospheric humidity was measured at 29.6, 18.3, 12.2, 7.6, and 2 m. Air temperature and humidity profile measurements were used to calculated changes in energy stored in air above the soil surface ($S$). Thermocouples also were positioned at 0.01, 0.05, 0.1, 0.2, 0.5, and 1.0 m below the soil surface to measure soil temperature. Volumetric water content was measured at the same depths at the soil thermocouples using horizontally installed water content reflectometers (Campbell Scientific, Logan, UT, model CS615) that were calibrated in the laboratory using soils from this location. Heat transfer in the soil was measured with a thermopile transducer (Radiation and Energy Balance Systems, Seattle, WA, model HFT-3.1) installed 7.5 cm below the surface.

Analog-to-digital signal conversion and data acquisition for all measurements at this site was accomplished with two data loggers (Campbell Scientific, Inc., Logan, UT, models CR10X and CR23X) connected to a notebook computer.

### 2.5. Turbulent and storage flux calculations

Fluxes of $CO_2$, latent heat (LE), and sensible heat ($H$) were calculated using methods described by

Berger et al. (2001). Half-hour fluxes were calculated from linearly detrended data after computing sonic-tube lag times, sonic rotation angle (based on an annual planar fit), and calibration coefficients for the $CO_2/H_2O$ analyzer. Throughout this paper, positive values indicate fluxes from the surface to the atmosphere.

Spectral corrections followed the methodology of Berger et al. (2001). Latent heat fluxes were spectrally corrected by mathematically degrading the temperature signal to match the observed $H_2O$ spectra, and multiplying the fluxes by the ratio of the non-degraded to degraded temperature flux (Goulden et al., 1996b). Degradation of the $CO_2$ spectra was not observed (see results section). It may exist, but if so it is masked by instrumental noise that dominates at high frequencies. Thus, a $CO_2$ spectral correction factor was computed based on the literature of flow through tubes and the characteristics of this apparatus. The correction factors that multiplied the uncorrected fluxes were about 1.01 and 1.2 for $CO_2$ and $H_2O$, respectively.

Storage fluxes were calculated from temporal changes in storage of $CO_2$, $H_2O$, and temperature between the soil surface and the height of the eddy flux measurement (29.2 m). Carbon dioxide mixing ratios from each sampling height were interpolated to produce 3 min time series that were vertically integrated to calculate storage within the air column. Aboveground heat storage was computed in the same manner using air temperature and water vapor measurements. There was insufficient data to accurately assess storage of heat in the standing biomass, so this component was not included in energy budget. Storage of heat in the soil ($G_s$) above the soil heat flux plate (0–7.5 cm) was calculated using the soil heat capacity ($C_s$) and the time rate of change in soil temperature:

$$C_s = \rho_b C_d + \theta_v \rho_w C_w \quad (1)$$

where $\rho_b$ is the soil bulk density ($1.3 \times 10^3$ kg m$^{-3}$), $C_d$ the heat capacity of dry soil (approximately $0.84 \times 10^3$ J kg$^{-1}$ K$^{-1}$), $\theta_v$ the volumetric soil water content (m$^3$ $H_2O$ m$^{-3}$ dry soil) at 5 cm below the soil surface, $\theta_v$ the density of water (approximately 1000 kg m$^{-3}$) and $C_w$ the heat capacity of water (approximately $4.19 \times 10^3$ J kg$^{-1}$ K$^{-1}$) and

$$G_s = \frac{\Delta T_s C_s d}{\Delta t} \quad (2)$$

where $\Delta T_s$ is the change in soil temperature (K) at 5 cm below the soil surface, $d$ the depth of upper soil layer (0.075 m), and $\Delta t$ the interval between soil temperature measurements (600 s). This storage term ($G_s$) was added to the soil heat flux density measurement to obtain total heat flux at the soil surface ($G$).

### 2.6. Data screening

Data were screened to eliminate instrumental error due to sensor limitations or interference by precipitation and condensation; methodological errors associated with micrometeorological conditions; and non-representative sampling of nighttime and early morning venting of pooled $CO_2$ from an isolated area within the forest. For humidity measurements greater than 100%, atmospheric humidity was calculated from saturated vapor pressure as a function of temperature. A leaf wetness sensor (Campbell Scientific, Inc., Logan, UT, model 237) was used to discard solar radiation measurements when moisture was present.

Micrometeorological conditions are not always suitable for measuring fluxes using the eddy covariance technique, especially during night when light wind conditions and near-surface temperature inversions restrict vertical mixing and may cause decoupling of the sub-canopy and overlying air (Mahrt et al., 2000). A storage term was used to account for the accumulation of $CO_2$ beneath the turbulence sensors (see above), but this was not always sufficient due to spatial heterogeneity within the forest, and weak horizontal winds beneath the canopy (Pattey et al., 1997). At this site, it was necessary to discard fluxes on the basis of low friction velocity ($u_* < 0.3$ m s$^{-1}$), and wind directions that reflected non-representative sampling conditions (90–180° from true north). Identification and selection of these screening criteria are discussed in the results section.

### 2.7. Quality control

The AmeriFlux relocatable reference system was collocated at this site during 18–21 July 2000. This roving system is used to detect deficiencies and validate the performance of long-term eddy covariance systems (http://public.ornl.gov/ameriflux/Standards/roving-system/roving_system.cfm). Measurements from

the two systems were highly correlated ($r > 0.91$) for $CO_2$, $H_2O$ vapor, and heat fluxes, and $CO_2$ fluxes agreed to within 4%.

### 2.8. Annual NEE, ER, and GEP calculations

Net ecosystem exchange (NEE) was computed by summing the spectrally corrected $CO_2$ flux, obtained by the eddy covariance method, and the $CO_2$ storage flux. Observed NEE was partitioned into photosynthetic and respiratory fractions to develop ecophysiological response functions that can be used to fill missing data gaps (e.g., Falge et al., 2001). Partitioning of NEE between gross ecosystem production (GEP) and ecosystem respiration (ER) was estimated using nighttime NEE rates, which integrate leaf dark respiration, plant construction and maintenance respiration, and heterotrophic respiration in the absence of photosynthetic uptake. Models of GEP and ER, and methods for obtaining annual cumulative NEE estimates are discussed below.

#### 2.8.1. Ecosystem respiration (ER) model

Forest primary production is returned to the atmosphere as $CO_2$, $H_2O$, and heat through respiration, a biological process whose reaction rates are primarily dependent on environmental conditions, especially temperature, and quantities of both living tissue and dead and decomposing organic matter. Tissue and substrate quantities are often ignored in studies of mature forest ecosystems, since the size of the total C pool does not change much on an annual time scale (Curtis et al., 2002). However, ecosystem carbon concentrations are essential for making site-to-site comparisons (e.g., Lloyd and Taylor, 1994) and regional scaling, which are over encompassing objectives of this and other studies. Biogeochemical reactions typically follow first-order kinetics, so the concentration dependency of ER can be written in the form of a first-order rate law:

$$\frac{dC_T}{dt} = -k_{ER} C_T \Rightarrow ER = -\frac{dC_T}{dt} = k_{ER} C_T \quad (3)$$

We fit this model using nighttime NEE as the ER rate (mol C $m^{-2}$ $s^{-1}$), where $C_T$ is the total carbon content of the forest stand ($1.518 \times 10^3$ mol C $m^{-2}$, including all woody vegetation and soil carbon to a depth of 30 cm; unpublished data), and $k_{ER}$ the rate constant ($s^{-1}$) for the reaction. The Eyring equation was used to describe the exponential response of $k_{ER}$ to temperature in terms of potential energy:

$$k_{ER} = \frac{k_b T_s}{h} e^{-\Delta G^{\ddagger}/RT_s} \quad (4)$$

where $k_b$ is the Boltzmann constant ($1.3806 \times 10^{-23}$ J $K^{-1}$), $T_s$ the soil temperature at 5 cm below the surface (K), $h$ the Planck's constant ($6.6262 \times 10^{-34}$ J s), $\Delta G^{\ddagger}$ the free activation energy (J $(mol\ C)^{-1}$) and $R$ the universal gas constant (8.3143 J $mol^{-1}$ $K^{-1}$). Soil temperatures were used for the depth that is most likely to contain the highest concentration of soil heterotrophic organisms and roots, since their growth and activity is primarily responsible for the belowground component flux that accounts for an estimated 74–88% of ER from this forest (Bolstad et al., 2004).

Free energy of activation is the potential energy that must be achieved by reactant molecules to form a transient product (Eyring, 1935), and its value provides quantitative information about the kinetics of a reaction. Enthalpic ($\Delta H^{\ddagger}$) and entropic ($\Delta S^{\ddagger}$) contributions to the free energy of activation were derived and calculated from Eq. (4) using the Gibb's free energy equation:

$$\Delta G^{\ddagger} = \Delta H^{\ddagger} - T\Delta S^{\ddagger} \quad (5)$$

and transforming the Eyring equation into a linear form to model ER:

$$\ln(k_{ER}) = \frac{ER}{C_T} = \ln\left(\frac{k_b T_s}{h}\right) + \frac{\Delta S^{\ddagger}}{R} - \frac{\Delta H^{\ddagger}}{RT} \quad (6)$$

where $k_{ER}$ is the observed respiration rate constant, and $\Delta S^{\ddagger}$ and $\Delta H^{\ddagger}$ the activation entropy and enthalpy, respectively. Plotting $\ln(k_{ER}h/k_b T_s)$ versus $(-(1/RT_s))$ yields a straight line with slope equal to $\Delta H^{\ddagger}$ and intercept equal to $\Delta S^{\ddagger}/R$. Eq. (6) was fit to half-hourly observations of $k_{ER}$ and $T_s$, using a 30-d moving window and fitting routine that minimizes the chi-square error statistic (LINFIT, Research Systems Inc., 1998). If the window contained fewer than 200 observations, window size was increased by 1 day until $n \geq 200$, but never beyond 43 days. Significance of model parameters (slope, intercept) were evaluated with a one-tailed $t$-test at the 90% confidence level, and mean respiration rates were used to fill data gaps if

a temperature dependent relationship was not observed.

Biological respiration within ecosystems can be modeled by numerous temperature response functions with considerable statistical success, and even a linear fit of log normal transformed rates and temperatures may provide enough accuracy to predict biological reaction rates over a narrow temperature range (e.g., Fang and Moncrieff, 2001). We chose to use the Eyring equation to model $k_{ER}$, because its theoretical construct allows us to derive meaningful parameters for site-to-site comparisons, regional scaling, and monitoring of seasonal and long-term trends. Eyring's equation is similar in form to the more commonly used Arrhenius equation, $k = A\,e^{-E_a/RT}$, but the later is based on empirical observations, and in a strictest sense only applies to gas reactions. Furthermore, it is easy to mistake the Arrhenius activation energy term ($E_a$) as the free energy of activation ($\Delta G^{\ddagger}$), when $E_a$ only contains information about the enthalpy component ($E_a = H^{\ddagger} + RT$).

#### 2.8.2. Gross ecosystem production (GEP) model

Using the ER model above, we estimated GEP as the difference between modeled ER and observed NEE during daylight hours. Photosynthetic parameters for estimating forest $CO_2$ uptake were obtained from a "big leaf" model that describes a response to quantum flux density (Ruimy et al., 1995):

$$-\mathrm{NEE} = \mathrm{GEP} - \mathrm{ER} = \frac{b_1 Q}{b_2 + Q} - b_0 \Rightarrow \mathrm{GEP} = \frac{b_1 Q}{b_2 + Q} \quad (7)$$

The parameters in this equation provide estimates of dark respiration ($b_0$), maximum assimilation rate ($b_1$) and photon flux density required for half saturation ($b_2$). We set ER = $b_0$ (as described in Eq. (6)) so that the intercept parameter of this non-linear equation was set to zero and only the light response variables, $b_1$ and $b_2$, were fit. Observed GEP and $Q$ data were fit to this function for each day of the year, using the same moving window technique and statistical methods as ER (see above). A fitting routine that uses the Levenberg–Marquardt algorithm was used to perform a non-linear least squares fit of the data (LMFIT, Research Systems Inc., 1998).

#### 2.8.3. Gap filling and annual cumulative NEE estimate

Equipment failures, interruptions during routine maintenance, and unfavorable weather conditions (i.e., precipitation or dew and frost formation on the sonic anemometer) encompassed 21% of all possible observations during 2000. Weak turbulence and non-representative sampling (discussed below) increased the number of missing observations to 50%, which is typical for most tower sites (Falge et al., 2001). Micrometeorological observations and GEP and ER models were used to fill missing half-hour measurements and estimate cumulative NEE. Although our method of using monthly averaged response functions cannot distinguish short-term acclimation of photosynthesis and respiration to temperature (e.g., Tjoelker et al., 2001; Gunderson et al., 2000; Larigauderie and Körner, 1995), it provides better spatial sampling and a statistically robust fit by including a wide range of temperatures. Short-term acclimation of water and carbon fluxes in forest vegetation has been shown to affect annual ecosystem sums by less than 10% (Kutsch et al., 2001a). Missing storage fluxes were filled using diurnal averages for the month. Data from 1999 included gaps of up to 1 month, so gap filling and annual NEE calculations were only performed for the 2000 calendar year.

## 3. Results and discussion

### 3.1. Environmental constraints

Climatic conditions during this 2-year study are presented in Fig. 2. Air temperatures during 1999 and 2000 were similar to long-term observations from Minocqua, WI, located about 50 km east of the site. With few exceptions, mean monthly air temperatures were within the range of data containing 80% of all monthly averages from 1905 to 2001 (National Climatic Data Center, Asheville, NC). Departures in air temperature included warm anomalies during November 1999 (+4 °C) and March 2000 (+3 °C), and a cool period during December 2000 (−6 °C). Annual cumulative precipitation at Minocqua, WI, during 1999 and 2000 was 86 and 83 cm, which was only slightly higher than the long-term average of 79 cm. Cumulative precipitation during May 1999 (20.0 cm)

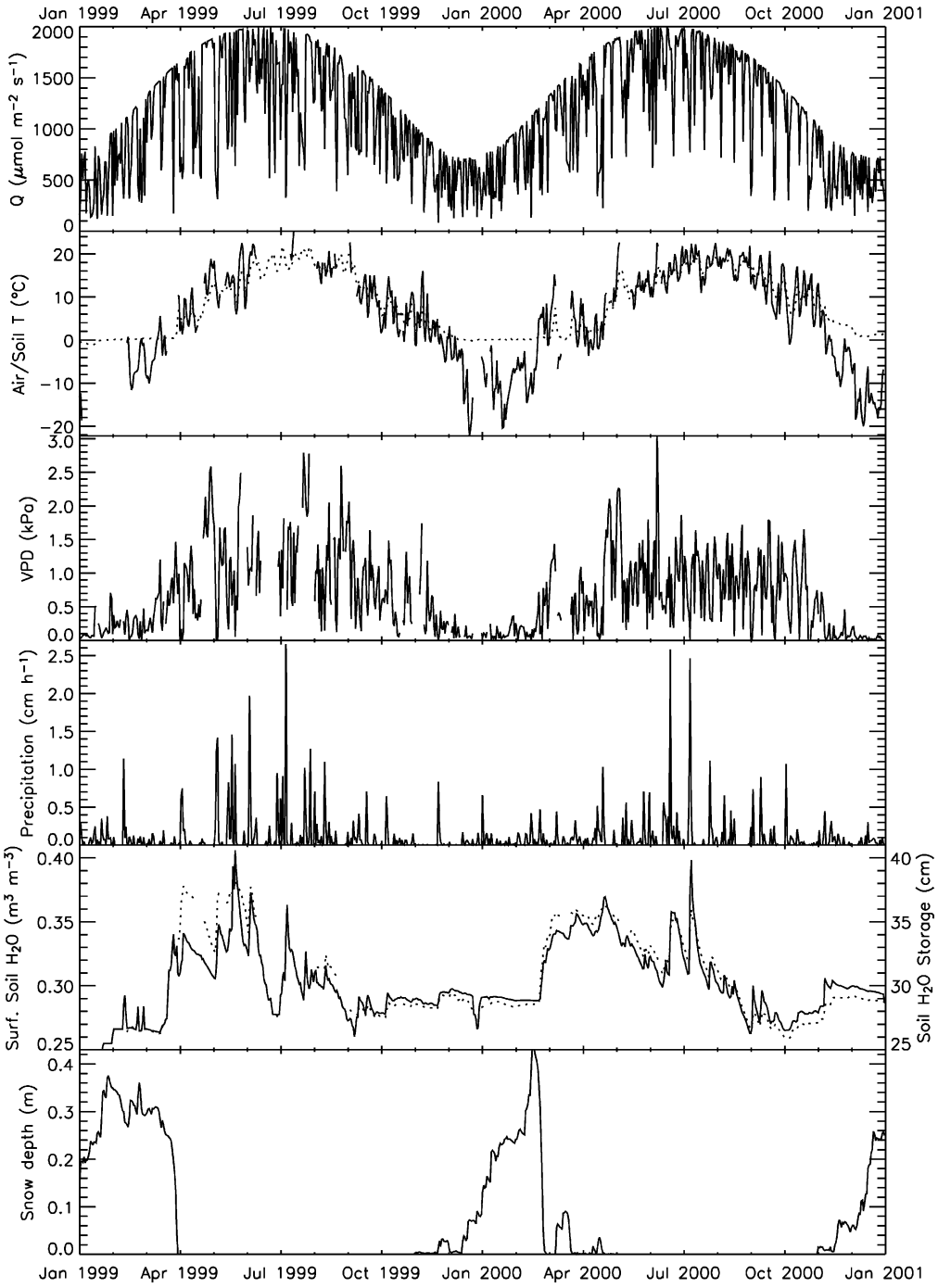


Fig. 2. Meteorological observations at or near the Willow Creek flux tower: (a) maximum daily photosynthetically active radiation ($Q$); (b) mean daily air temperature at 29.6 m above the soil surface (solid line), and mean daily soil temperature at 5 cm below the soil surface (dashed line); (c) maximum vapor pressure deficit near the canopy top (20.3 m); (d) mean water equivalent precipitation rates; (e) mean daily soil moisture content at 20 cm below the soil surface (solid line), and mean daily soil water integrated to 1 m below the soil surface; (f) mean daily snow depth.

was the greatest on record for that month, and cumulative precipitation during July of both years was almost two times greater than the long-term average (10.5 cm). Abundant rainfall during the first half of the 1999 and 2000 growing seasons was offset by less than average precipitation during the fall (September–November) of both years. Annual precipitation at this site was similar to other deciduous and mixed deciduous forests where carbon and water fluxes are being measured (Harvard Forest, MA; University of Michigan Biological Station, MI; Camp Borden, Ontario), but annual and mid-summer air temperatures were about 1–3 °C lower.

### 3.2. Low-turbulence threshold

Micrometeorological conditions were not always suitable for measuring fluxes using the eddy covariance technique, especially during night when light wind conditions and near-surface temperature inversions restricted vertical mixing. Storage fluxes were included in the NEE calculation to reduce errors associated with turbulent fluxes, but significant bias can still occur due to drainage of cold surface air (e.g., Anthoni et al., 1999). Observations from the Willow Creek flux tower were segregated by friction velocity ($u_*$) and used to identify a threshold value below which NEE measurements were significantly less than monthly averages (Fig. 3). A $u_*$ threshold of 0.3 m s$^{-1}$ was observed at this site, which was similar to values used at other forested locations (Schmid et al., 2000, 2003; Goulden et al., 1996b; Aubinet et al., 2000; Falge et al., 2001). About 14% of the observations from 1999 and 2000 were discarded on this basis, which was somewhat less than most sites (Falge et al., 2001). Removal of low-turbulence data had a relatively small effect on annual NEE, which is discussed below.

### 3.3. Anomalous venting events

Based on observations from multiple years, we have hypothesized that the area to the SE of the Willow Creek flux tower is susceptible to nighttime and early morning venting of stable layers of air near the soil surface, which are characterized by high concentrations of $CO_2$ from either local respiration or cold-air drainage into low-lying areas. To our knowledge, this phenomenon has not been observed or

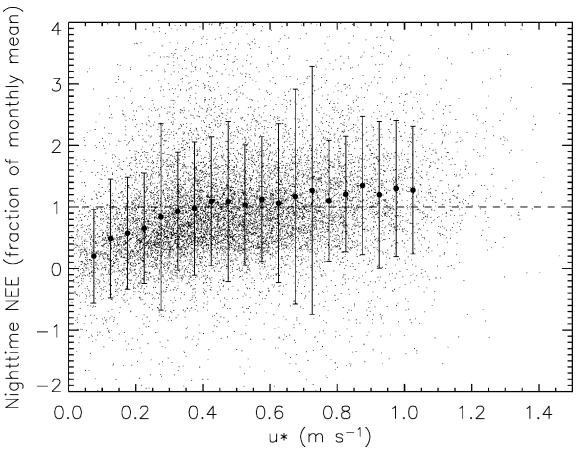


Fig. 3. Normalized nighttime NEE as a function of $u_*$ at the Willow Creek tower (long-term data from 1999 to 2002, excluding wind directions from that were associated with venting anomalies). Solid circles with error bars represent means and standard deviations of data binned by $u_*$ in increments of 0.05 m s$^{-1}$.

documented at other flux tower sites. It was an unexpected finding for a seemingly homogenous forest stand like Willow Creek, and in the sections that follow, we have isolated and characterized flux data and micrometeorological conditions that validate and describe these events. Unique features and site specific information allowed us to form hypotheses that would explain the mechanisms responsible for these venting events, which in turn provided the rationale for screening these data.

#### 3.3.1. Characteristics of venting anomalies

Localized venting of $CO_2$ was initially suggested by unusually high nighttime and early morning NEE measurements, some as high as 80 μmol $CO_2$ m$^{-2}$ s$^{-1}$, from an isolated wind direction SE of the tower (Fig. 4). We refer to these events as venting 'anomalies', because highly positive turbulent flux measurements, often sustained for several hours at a time, were only partially compensated by changes in $CO_2$ storage. The magnitude of these anomalous NEE measurements increased with soil temperature and decreased when soil moisture exceeded about 0.35 m$^3$ m$^{-3}$ (data not shown), suggesting a biological source such as microbial respiration from soils. However, direct soil surface flux measurements from numerous locations within the tower footprint during the same period were consistently less than

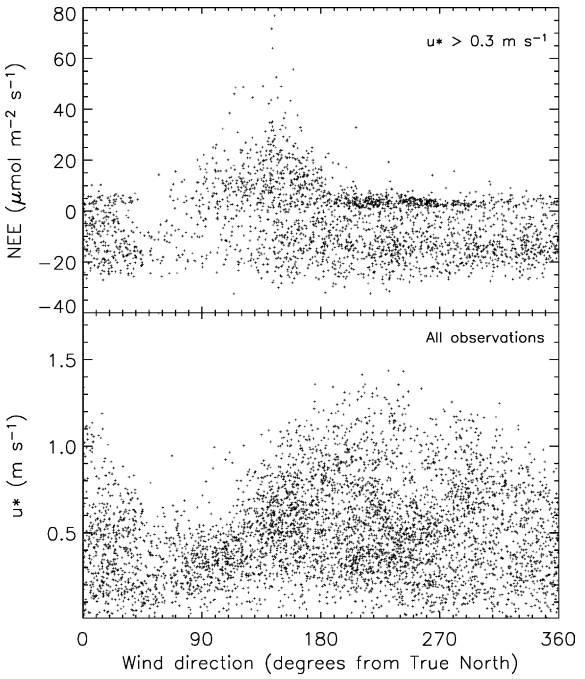


Fig. 4. Net ecosystem exchange (NEE) from 1999 and 2000 growing seasons, showing (a) exceptionally large respiration fluxes from the SE quadrant during valid turbulent conditions ($u_*$ >0.3 m s$^{-1}$) and (b) reduced friction velocities ($u_*$) associated with local topography and higher elevations to the east.

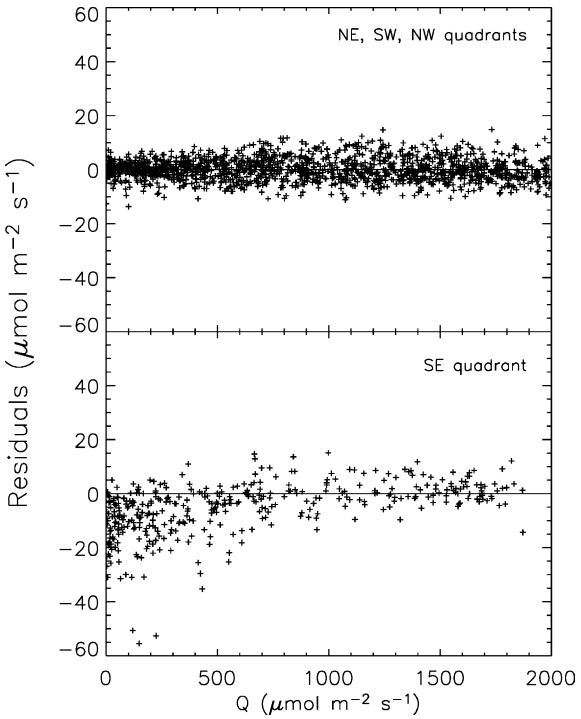


Fig. 5. Residuals of modeled daytime NEE from June to August 2000. Distribution of residuals around zero confirmed nighttime NEE measurements (i.e., $b_0$ in "big leaf" GEP model) provided accurate estimates of daytime ER; skewed residuals from the SE during early morning hours were associated with venting anomalies.

8 μmol $CO_2$ m$^{-2}$ s$^{-1}$ and belowground respiration accounted for about 80% of the ER at this site (Bolstad et al., 2004).

Anomalous NEE measurements from the SE quadrant were observed during the early morning hours also. Residuals of modeled NEE were normally distributed around zero throughout the daytime for all directions but the SE quadrant (Fig. 5). In the SE quadrant, residuals were negatively skewed during the early morning hours under low light conditions ($Q <$ 500 μmol m$^{-2}$ s$^{-1}$), and normally distributed during the middle of the day when vigorous convective turbulence was expected. In a homogenous forest such as Willow Creek, this seemed to suggest that respiration and photosynthesis in the SE quadrant was similar to other directions during midday when sub-canopy $CO_2$ storage was low and convective turbulent conditions were adequate. This also suggested a strong respiratory source within the larger nighttime and early morning flux footprint, such as low-lying depressions and distant wetlands to the SE and S (Fig. 1). Venting events greater than 20 μmol m$^{-2}$ s$^{-1}$ from the SE were characterized by steady and moderately high wind speeds above the forest canopy (2.5 ± 0.98 m s$^{-1}$, mean ± S.D.), which indicated either a distant source or greater shear production (i.e., stronger turbulence and deeper penetration into the forest sub-canopy).

### 3.3.2. Validity of measurements during venting anomalies

The magnitude of the anomalous NEE observations raised questions about the validity of flux measurements during these events. Their validity was confirmed using friction velocity ($u_*$), time series, and spectral data. Data from a 10-day period in August 2003 is presented in Figs. 6–8 to illustrate two separate venting events at Willow Creek, and compare above-

canopy measurements with an on-site sub-canopy flux system and two nearby AmeriFlux towers. Net ecosystem exchange at Willow Creek during nighttime and early morning venting (days 224 and 229) was characterized by a large respiratory signal in the turbulent flux measurements (Fig. 6), which was not associated with weak turbulence (represented by $u_*$, Fig. 7), pooling of cold air and $CO_2$ near the tower at night (Fig. 6), or early morning transition to convective conditions (e.g., Lost Creek on days 231 and 232). It is worth noting that elevated fluxes were sustained for several hours during venting events, which is noticeably different from random fluctuations (both positive and negative) that are observed during low turbulence (e.g., days 226, 231, and 232).

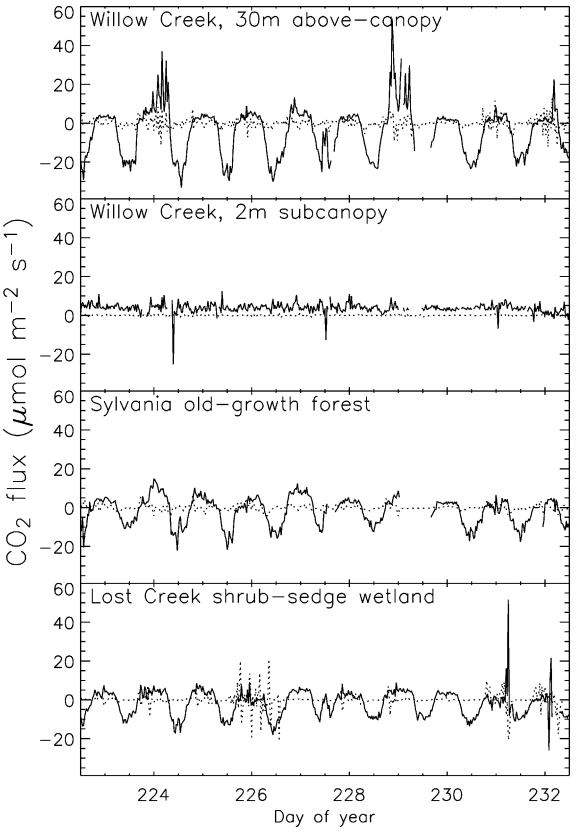


Fig. 6. Eddy covariance (solid line) and storage flux (dotted line) observations from four stations near the above-canopy tower at Willow Creek during August 9–20, 2002. Nighttime and early morning venting events on days 224 and 299 were unique to Willow Creek, and appeared only in the eddy covariance measurement above the forest canopy.

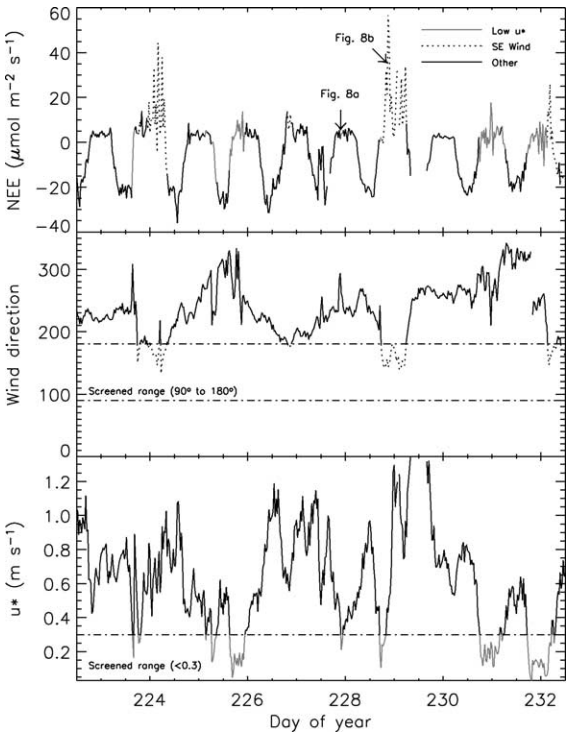


Fig. 7. Above-canopy NEE measurements and micrometeorological conditions at Willow Creek (August 9–20, 2002) that were used to screen data for weak turbulence ($u_* < 0.3$ m s$^{-1}$; gray line) and non-representative sampling conditions (SE winds; dotted line). Nighttime and early morning venting anomalies from the SE quadrant were not associated with weak turbulence; venting events lasted several hours; and elevated fluxes during venting could be differentiated from random signal noise associated with weak turbulence.

The anomalous venting did not appear to penetrate deep into the canopy (e.g., Mahrt, 1985; Baldocchi and Meyers, 1991), or represent a strong local soil source since above-canopy events often lasted several hours without being observed by a 2 m sub-canopy flux system (Fig. 6) located just 50 m from the tower. Sub-canopy fluxes were measured with a CSAT sonic anemometer and open-path infrared gas analyzer (Li-Cor, Lincoln, NE, model LI-7500) at a height of 2 m above the soil surface.

No other flux tower in the region observed similar anomalous fluxes (Fig. 6), providing additional support for a site specific phenomenon. Storms and synoptic fronts are often associated with winds from the south and east, and these systems can cause strong mixing of the boundary layer and troposphere,

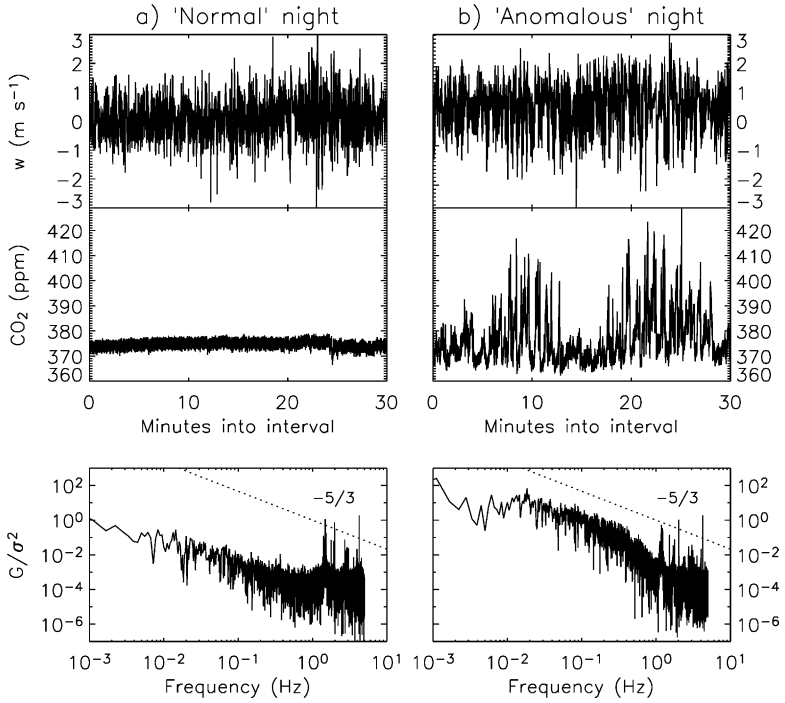


Fig. 8. Fast (10 Hz) time series of vertical velocity ($w$) and $CO_2$ mixing ratio, and normalized $CO_2$ spectra for sequential nights in August 2000 (see Fig. 7) during which (a) venting was not observed, and (b) venting was observed.

horizontal advection, wind gusts, and dramatic changes in atmospheric pressure. If these rapidly changing conditions violated assumptions of the eddy covariance method (e.g., a non-stationary atmosphere) or barometric or wind-induced pressure variations enhanced efflux of $CO_2$ from soils (e.g., Baldocchi and Meyers, 1991), we would expect to observe similar anomalies at other flux towers in the region. The Sylvania old-growth forest and Lost Creek shrub wetland are located within 100 km of Willow Creek, but neither demonstrated anomalous fluxes from the SE or any other wind direction (Fig. 6).

Time series of 10 Hz vertical velocity ($w$) and $CO_2$ mixing ratio measurements were extracted for sequential nights in August 2002 to compare turbulence and scalar transport during 'normal' and 'anomalous' nights (Fig. 8). There was no indication of instrument anomalies (e.g., data spikes) or evidence of non-stationary conditions (e.g., dramatic shifts in the mean value during the half-hour averaging period) during these periods that would violate assumptions of the eddy covariance calculations. Vertical velocities (Fig. 8) and $u_*$ (Fig. 7) were typically higher during (and prior to) venting anomalies, and suggesting greater turbulence during venting. Normalized $CO_2$ spectra from both time periods showed a demonstrated that a 30 min average time was satisfactory on both occasions, since the sampling period was long enough to capture a range of frequencies (i.e., eddy sizes) that were characterized by a $-5/3$ slope typical of atmospheric turbulence, rather than a white noise spectrum that might exist if the data were dominated by instrumental noise or spikes.

### 3.3.3. Mechanisms attributed to venting anomalies

On most nights, including all those in Figs. 6-8, gradient Richardson numbers above the forest canopy indicated dynamic stability ($R_i > 1.0$) and decoupling of the sub-canopy and atmosphere above (data not shown). In forests with closed canopies, these conditions develop by rapid radiative cooling and formation of a strong temperature inversion layer at the canopy top (Mahrt et al., 2000). Tower flux measurements require that transport is one-dimensional and that storage and eddy-covariance fluxes be representative of similar areas (Yi et al., 2000). Decoupling of the above and sub-

canopy flow elevates the potential that these conditions are violated. We hypothesize that these assumptions are often violated at Willow Creek during the nighttime and early morning when winds were from the SE. We further hypothesize that this quadrant exhibits a greater tendency for pooling of $CO_2$ than other wind directions.

Since venting events often lasted for several hours at a time, either the reservoir of pooled $CO_2$ or the area being vented must be quite large. Ground and aerial observations within the flux footprint (Fig. 1) revealed similar vegetation and soils to the SE as compared to other directions, and there were no large gaps or discontinuities in the forest canopy that might create conditions for venting induced by a windbreak. The path taken by the largest venting anomalies generally runs parallel to local topography, and before reaching the tower, flows over some depressions near the edge of the nighttime flux footprint and along the toe slope of a small hill to the east (Fig. 1). The depressions represent areas where $CO_2$ from higher elevations might pool due to cold-air drainage at night. Terrain driven advection (i.e. cold-air drainage) might permit a supply of respired $CO_2$ from a large area to be concentrated in a smaller area during stable conditions, and pooled $CO_2$ would be vented when above-canopy winds were sufficiently strong to penetrate the stratified layer above the forest canopy.

Farther away from the tower (0.6–1.3 km) were more expansive low-lying areas, wildlife openings, roadways, and wetlands (Fig. 1) that also may have contributed to preferential pooling and venting of $CO_2$. Low-lying areas have the potential to be a greater source of $CO_2$ than forested uplands, because soil organic matter content is often higher in lowlands, and respiration rates can be greater if aeration is not limited by excess soil moisture. In addition, strong nighttime inversions do not always form over open canopies, and stable layers in the sub-canopy may break down under lower $u_*$ thresholds (Mahrt et al., 2000). It would seem improbable, however, that a turbulence signal could reach the flux tower over these distances. The roughness transition between wetland and forest vegetation can generate turbulence that has been observed as far away as 25 times the measurement height ($z_m$; Irvine et al., 1997), but the nearest wetland to the Willow Creek tower was about twice this distance (Fig. 1). Thus, it seemed unlikely that any turbulence generated in the vicinity of these distant sources would be detected at the Willow Creek tower. An alternative hypothesis is that relatively high winds and strong stability permitted $CO_2$ to reach the tower as stratified layers above the forest canopy, and at a point fairly close to the tower, laminar flow became turbulent due to local changes in stability, wind speed, or surface roughness. Flow through the tower structure was not likely to play a role in these flux events since it was located to the NE of the sonic anemometer, neither up- or downwind of the anomalous fluxes.

#### *3.3.4. Errors associated with venting anomalies*

Only ~3% of all NEE observations exceeded an arbitrary ER threshold of 10 μmol $CO_2$ $m^{-2}$ $s^{-1}$, but the magnitude of these observations and skewing of ER and GEP models fits had a substantial effect on the annual cumulative flux. Cumulative ER was increased by 317 g C $m^{-2}$ $year^{-1}$ when models included data from SE quadrant, which would be enough to change this forest from a moderate sink (discussed below) to nearly neutral with respect to NEE of $CO_2$.

We have demonstrated that turbulence measurements during anomalous flux events were valid, and we postulated that these anomalies resulted from preferential pooling or venting in the area to the SE. Assuming the problem is primarily attributed to preferential venting, either within the forest or from distant wetlands, we would want to discard these data on the basis of non-representative sampling; i.e., the turbulent flux footprint encompassed a very large drainage area, or included fluxes not representative of the local forest stand. The only rationale for keeping these anomalous observations would be an argument that these anomalous flux events somehow compensated for drainage that goes on undetected at the tower during other times of the year.

Screening data for low turbulence and winds from the SE (90–180° from true north) removed 14 and 15% of the observations, respectively, but increased our confidence that systematic errors in the annual carbon budget were minimized. After screening, we observed that sub-canopy fluxes agreed in magnitude with nighttime above-canopy NEE measurements (Fig. 6). Despite these assurances, we could not explain apparent discrepancies between tower fluxes and respiration estimates that were scaled from component fluxes (Bolstad et al., 2004). Convergence of tower- and component-based estimates of ER has difficult to

achieve at other sites as well (Dore et al., 2003; LaVigne et al., 1997; Goulden et al., 1996a). We are currently addressing this concern at Willow Creek by developing respiration models that incorporate soil moisture, and analyzing sub-canopy fluxes and wind profile data for evidence of $CO_2$ advection.

### 3.4. Surface energy balance

Achieving closure of the energy budget ($(H + LE)/(R_n - G - S) \equiv 1$) is important for calculating and interpreting surface energy partitioning, and validating the $CO_2$ and $H_2O$ flux calculations (Verma et al., 1995; Moncrieff et al., 1997). The overall energy balance for this site was 72%, which was calculated using an algorithm that fits a straight-line model to data with errors in both $x$ and $y$ coordinates (FITEXY, Press et al., 1992). Screening data for low-turbulence conditions did not balance the surface energy budget, and similar lack of closure occurred during both daytime and nighttime periods.

A synthesis of eddy covariance data from 22 FluxNet towers demonstrated similar energy imbalances and relationships with turbulence (Wilson et al., 2002). Errors associated with the eddy covariance method are at least partially responsible for the lack of energy balance closure, and Wilson et al. (2002) provided evidence that the magnitude of NEE across many sites was reduced when energy closure was poor. This possible link between scalars that are measured by eddy covariance has prompted some researchers to suggest that NEE measurements should be corrected on the basis of energy budget errors (Twine et al., 2000). We have not attempted this at Willow Creek, since it was equally possible that energy imbalances could have resulted from errors in available energy measurements or neglecting heat storage in biomass (Wilson et al., 2002; Mahrt, 1998).

### 3.5. Ecosystem respiration (ER) and seasonal trends

Average nighttime NEE observations peaked at 6 $\mu mol\ m^{-2}\ s^{-1}$ during mid-July, and were suppressed (0.1–1 $\mu mol\ m^{-2}\ s^{-1}$) during periods of snow cover (Fig. 2). This range of observed rates is similar to other deciduous forests from the EUROFLUX and AmeriFlux networks (Falge et al., 2002), including a northern hardwood forest in northern lower Michigan (Schmid et al., 2003). Free energy of activation ($\Delta G^{\ddagger}$) was used to model ER during 2000 (Fig. 9), and provide quantitative information about the kinetics of respiration. An attempt was made to determine individual contributions of enthalpy ($\Delta H^{\ddagger}$) and entropy ($\Delta S^{\ddagger}$) to $\Delta G^{\ddagger}$, but variations appeared to be linked to sample size and goodness-of-fit statistics (i.e., propagation of experimental errors; Cornish-Bowden, 2002; Krug et al., 1976) and failed to suggest any biological significance.

Seasonal variations in $\Delta G^{\ddagger}$ include the effects of temperature, soil moisture, substrate availability, plant growth, and microbial activity on ER rates. During winter when snow cover was present, we observed that ER was insensitive to temperature (i.e., model parameters were not significant), and mean nighttime NEE was used to fill gaps in ER. Ecosystem respiration was much lower and more difficult to detect during this time, and meaningful relationships may have been complicated by decoupling of above- and belowground systems. Insulating properties of the snow cover minimized the soil heat flux and held soils at temperatures slightly above freezing, while air and stem temperatures were often 10–20 °C lower (Fig. 2).

From early spring until the onset of leaf senescence (mid-August), $\Delta G^{\ddagger}$ steadily increased with soil temperature. This observation is noteworthy, because temperature alone would be expected to have a negative affect on $\Delta G^{\ddagger}$. Higher activation energies can be interpreted as an increase in the amount of energy that must be initially expended to break and form chemical bonds at a specific temperature, and

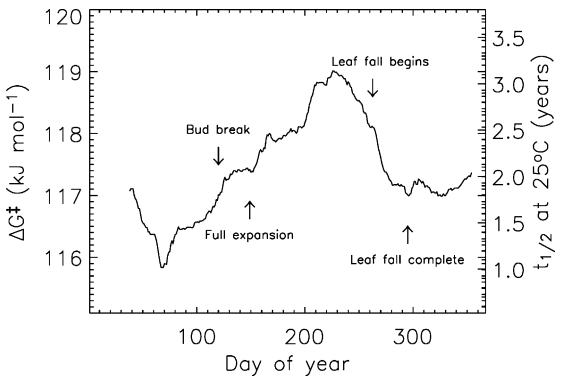


Fig. 9. Changes in ecosystem respiration model parameters and half-life estimates ($t_{1/2}$ at standard temperature) for the Willow Creek carbon pool during 2000.

generally relate to lower reaction rates. Soil water was decreasing during this time (Fig. 2), which could explain initial increases but not subsequent decreases. Also, soil moisture contents remained high throughout 2000, ranging from 0.26 to 0.40 $m^3\ m^{-3}$, and according to chamber soil efflux measurements seemed to be less important than temperature for predicting belowground respiration. Enhanced root growth and leaf-out during the spring would be expected to lower $\Delta G^{\ddagger}$ early in the year expansion (Wilson et al., 2001; Law et al., 1999; Ryan et al., 1997), but distinctive surges were not observed during bud break and canopy development. It seemed more likely that seasonal variations of $\Delta G^{\ddagger}$ reflected the availability of labile C in litter fall. Heterotrophic respiration represented about 38% of the annual respiratory flux from Willow Creek (Bolstad et al., 2004), and we would expect a strong signal associated with the progressive decomposition of litter from the previous autumn. Increases in $\Delta G^{\ddagger}$ during the growing season would reflect losses of available substrate and utilization of more recalcitrant carbon, while a rapid decrease in the fall would accompany senescence and new litter fall.

Modeled reaction rate constants were converted to reactant half-life, i.e., time required for the concentration of a substrate to decrease by 50% ($t_{1/2}$), as follows:

$$t_{1/2} = \frac{\ln(2)}{k_{ER}} \quad (8)$$

Half-life estimates for Willow Creek ranged from about 1 to 3 years at 25 °C, which seemed to agree with inversion model estimates for non-woody litter (1.1 years), and the more recalcitrant structural component of this pool (2.2 years; Luo et al., 2003).

### 3.6. Gross ecosystem production (GEP) and light response functions

Intercepted $Q$ by the forest canopy was used to determine phonological dates for bud break (29 April), full leaf expansion (28 May), beginning of leaf fall (26 September), and completion of leaf fall (21 October) during the 2000 growing season. Peak photoassimilation (i.e., maximum light response and light saturation) occurred from June to August (Fig. 10). Maximum assimilation rates increased after full leaf

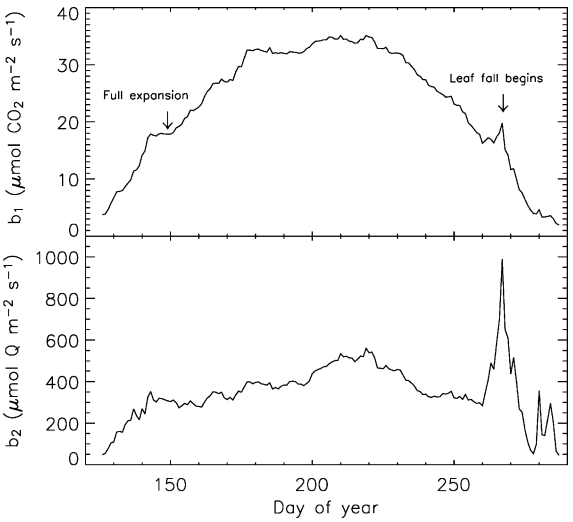


Fig. 10. Changes in photosynthesis model parameters, maximum assimilation rate ($b_1$) and photon flux density required for half saturation ($b_2$) for Willow Creek during 2000.

expansion until the summer solstice, indicating that both leaf area and sun angle were important variables for predicting carbon uptake rates during the spring. For a brief period (<1 week) prior to the beginning of leaf fall, GEP demonstrated a sudden decrease in light sensitivity (i.e., increase in photon flux density required for half saturation, $b_2$; Fig. 10). This conspicuous change in light response was almost certainly associated with decreased chlorophyll production and increased synthesis of anthocyanin by the leaves. Subsequent reductions in GEP and model parameters were associated with loss of the canopy, as evidenced by a decrease in intercepted $Q$ (data not shown).

Maximum rates of carbon assimilation were greater than most forests types selected from the EUROFLUX and AmeriFlux networks by Falge et al. (2002), but similar to another cold upland deciduous forest in the northern Great Lakes region (Schmid et al., 2003). Falge et al. (2002) noted that the amplitude of GEP rates was characteristically higher in forests with shorter carbon uptake periods, such as Willow Creek. Light response and respiration coefficients were somewhat less than those reported by Lee et al. (1999) for Camp Borden, a deciduous forest located at similar latitude in southern Ontario, Canada. In contrast to Willow Creek, the rapidly growing forest

at Camp Borden is largely composed of mid-succession species, *A. rubrum*, *Populus tremuloides* and *Fraxinus americana*. The comparison between sites highlights the importance of species composition and stand age on photosynthetic uptake and variability within broad latitudinal bands.

Maximum incoming radiation for photosynthesis ($Q_{max}$) was estimated for each half-hour interval (Bird and Hulstrom, 1981) in order to separate clear skies ($Q/Q_{max} > 90\%$) from cloudy, hazy, or overcast skies ($Q/Q_{max} < 90\%$). Sky conditions can affect light quality and meteorological conditions (e.g., VPD and leaf temperatures), and influence photosynthetic light response curves (Gu et al., 1999; Law et al., 2002). As previously documented at other sites, maximum carbon uptake was lower (i.e., NEE was higher) under clear skies (Fig. 11). During July 2000, sky conditions had a 2–3 μmol $m^{-2}$ $s^{-1}$ effect on NEE at $Q > 500$ μmol $m^{-2}$ $s^{-1}$, emphasizing the need to incorporate this environmental variable into more sophisticated models of carbon exchange.

### 3.7. Annual sums of NEE and ecological inventory estimates

Annual NEE was estimated for 2000 only, because gaps during January and June/July of 1999 were too large to fill with confidence. Annual sums of gap-filled and modeled NEE amounted to −334 and −348 g C $m^{-2}$, respectively, providing confidence in gap-filling methods and indicating that this upland forest stand was a moderate sink for $CO_2$. Screening for weak turbulence had a small effect on annual NEE, increasing the cumulative total from −355 to −334 g C $m^{-2}$. This correction is much lower than estimates for a broadleaf deciduous forest in hillier terrain, which showed a difference in annual NEE of 240 g C $m^{-2}$ $year^{-1}$ (Schmid et al., 2000), and suggested that advection during calm conditions is not as problematic at this site.

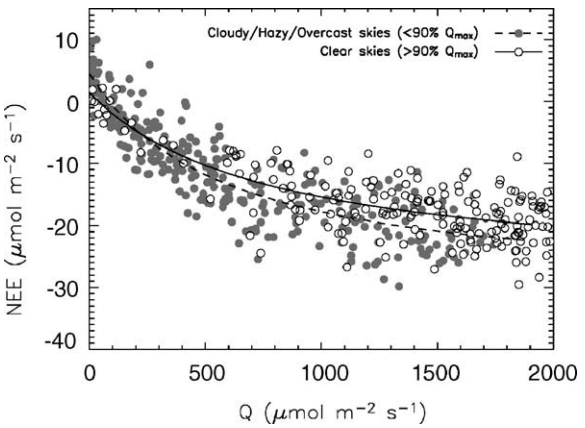


Fig. 11. Increased $CO_2$ uptake rates associated with cloudy, hazy, and overcast sky conditions during July 2000.

Annual net uptake of carbon at Willow Creek was greater than has been observed at Harvard Forest, University of Michigan Biological Station, and Camp Borden, where annual NEE typically ranges from 140 to 310 g C $m^{-2}$ $year^{-1}$ (Goulden et al., 1996a; Baldocchi et al., 2001; Schmid et al., 2003; Lee et al., 1999; Ehman et al., 2002). These sites are all deciduous forests within the same latitudinal band, but show distinct differences in species composition, soil characteristics, land use history and local climatic conditions. In each case, recovery from past disturbance is the likely cause of net uptake of carbon from the atmosphere by these forests (Caspersen et al., 2000; Post and Kwon, 2000).

The importance of these results is emphasized by large-scale measurements from WLEF, the 447 m tall tower located about 22 km NW of the Willow Creek flux tower (Davis et al., 2003). Observations at WLEF integrate fluxes from many land cover types, including upland deciduous forest similar to that surrounding the Willow Creek tower. Both sites are located in the same geographical region and exposed to the same climatic conditions, and estimates of cumulative NEE at WLEF in 1997 (+16 g C $m^{-2}$ $year^{-1}$; Davis et al., 2003) and subsequent years (55–147 g C $m^{-2}$ $year^{-1}$, unpublished data) indicate that the local landscape is close to carbon balance with or a modest carbon source to the atmosphere. The forest surrounding these towers is heavily managed. Land use history is typically correlated with species composition and soil type in northern Wisconsin (Cole et al., 1999; Curtis, 1959). Land use history, species composition and soil characteristics may explain the differences between NEE at these tower sites. Reconciling these differences will be an important step towards up-scaling flux tower data to larger regions.

Biometric and ecoyphysiological measurements were used to compute forest net primary production (NPP) and net $CO_2$ exchange independent of the eddy

covariance observations following the methods of Clark et al. (2001) and Ehman et al. (2002). Annual estimates of aboveground NPP were based on stem growth increments, tree diameters, and allometric equations (Ter-Mikaelian and Korzukhin, 1997) to obtain an average growth rate during the previous 3–5 years (unpublished data). Belowground respiration for 2000 was estimated from soil chamber flux measurements and temperature and moisture response functions (Bolstad et al., 2004; unpublished data). Assuming that belowground NPP was 20% of the aboveground NPP (Gower et al., 2001) and heterotrophic respiration accounted for 50% of the belowground $CO_2$ efflux (Hanson et al., 2000; Zogg et al., 1996), we estimated Willow Creek NEP was 188 g C $m^{-2}$ (Table 1), which is 44% less than the tower-based NEE. Curtis et al. (2002) observed that biometric estimates differed from tower-based NEE by 35–325 g C $m^{-2}$ in four other North American deciduous forests, and argued that different periods of data collection and errors and uncertainties in biometric and eddy-covariance methods may contribute to these differences. Barford et al. (2001) found good agreement with a 10-year comparison of NEP and NEE at Harvard Forest, but comparisons for individual years were poor due to temporal dynamics of the forest carbon cycle (e.g., lagged response to detritus inputs and environmental stress).

### 3.8. Carbon partitioning and turnover

Net ecosystem exchange can be partitioned between ER and GEP (Fig. 12), and seasonal patterns and annual sums may help us identify and better understand inter-annual variability and site-to-site differences (Falge et al., 2002). In springtime, both GEP and ER increased shortly after the snow cover disappeared and mean soil temperatures warmed to $>10\ ^{\circ}C$ (Fig. 1). This is consistent with post-winter recovery of other tree species growing at high latitudes (Bergh and Linder, 1999; Lee et al., 1999), and evidence that belowground respiration is largely driven by warmer bulk soils (Russell and Veroney, 1998) and increased availability of photoassimilates in rhizosphere soil (Högberg et al., 2001). Falge et al. (2002) suggested that ER lags slightly behind GEP during the spring in temperate deciduous forests, but we observed the opposite trend. The highest ratios of ER:GEP occurred during leaf expansion and senescence, with ER outpacing GEP by as much as a factor

Table 1
Estimated annual net carbon exchange and component estimates (g C $m^{-2}$ $year^{-1}$) for the Willow Creek upland hardwood stand. Herbivore, leaching, and volatilization losses were not included in these estimates

| Measurement | Method/reference | Estimate |
|---|---|---|
| Change in biomass | | |
| Boles and branches | Stem cores, dbh[a]; allometric equations[b] | 162 |
| Stump and roots | (Boles and branches) × 0.2[c] | 32 |
| Detritus production | | |
| Aboveground | Litterfall[a] | 133 |
| Belowground | Root standing stock and turnover rates[d] | 384 |
| Heterotrophic respiration | | |
| Forest floor and soil | Chamber model[d] minus root respiration[e,f] | −444 |
| Coarse woody debris | Chamber model and ground survey[a] | −79 |
| Net exchange | | |
| NEP | Inventory (sum of above)[g] | 188 |
| NEE (2000) | Flux tower (this paper) | −334 |

[a] J. Martin (unpublished data).
[b] Ter-Mikaelian and Korzukhin (1997).
[c] Gower et al. (2001).
[d] Bolstad et al. (2004).
[e] Zogg et al. (1996).
[f] Hanson et al. (2000).
[g] Clark et al. (2001).

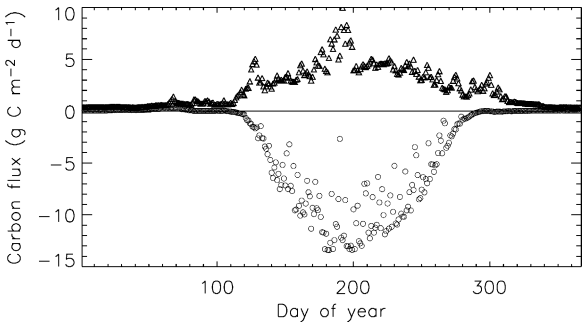


Fig. 12. Daily partitioning of NEE between gross photosynthesis (circle) and ecosystem respiration (triangle) at Willow Creek during the period between full canopy development and leaf senescence, 2000.

of 10. Net ecosystem exchange was relatively low during these 2-week transitional periods, because bulk soil temperatures were low. Daily ER:GEP ratios averaged about 0.5 during the rest of the growing season days, and 0.7 during the entire year. These observations suggest that the occurrence and timing of soil freeze/thaw, snow pack development, and canopy duration will be critical determinants in inter-annual variability at this site (Brooks et al., 1997; Savage and Davidson, 2001; Goulden et al., 1996a).

Annual sums of modeled ER and GEP during 2000 were 817 and 1165 g C m$^{-2}$, which represented mid-range values for deciduous forests selected from the EUROFLUX and AmeriFlux networks by Falge et al. (2002). Estimates of annual GEP were nearly identical to another upland hardwood forest site in the Great Lakes region during 1999 (University of Michigan Biological Station; 1350 g C m$^{-2}$), but ER was much lower than the Michigan site (1180 g C m$^{-2}$; Schmid et al., 2003). From the total pool size and annual ER, we calculated a carbon turnover time of 22 years for Willow Creek.

Compared with landscape-scale measurements at the WLEF tall tower, photosynthesis rates were consistently higher and annual photosynthetic uptake was about 25% greater at Willow Creek during 2000 (Cook et al., 2001). The flux footprint at WLEF includes less productive wetlands and recently logged or thinned forest, and may explain lower photosynthetic fluxes. In contrast to photosynthetic uptake, respiration rates during 2000 were higher at WLEF, resulting in annual respiration fluxes that were about 23% greater than at Willow Creek. Differences in respiration may be related to seasonal fluctuations in surface water depth and temperatures of wetland soils; ER rates at WLEF were the highest in July and August, when $T_s$ was the highest and surface water depth was the lowest in nearby wetlands (Cook et al., 2001). Belowground respiration can be enhanced by as much as two orders of magnitude when the water table is lowered, as has been observed in wetland drainage experiments (Silvola et al., 1996), root growth studies (Kutsch et al., 2001b), soil incubations (Updegraff et al., 1995), ecosystem models (Savage and Davidson, 2001), and eddy covariance measurements (Lafleur et al., 1997).

### 3.9. Forest evapotranspiration and relation to $CO_2$ exchange

Forest evapotranspiration is regulated by solar radiation, vegetation, atmospheric humidity, wind, and plant water availability. Soil water holding capacity was high at this site, and soil water contents were consistently high throughout this study (Fig. 2). Prior to leaf emergence in spring, $H$ increased dramatically (Fig. 13) due to increased incoming radiation and disappearance of snow cover (Fig. 2). Latent heat fluxes increased rapidly during May and June (Fig. 13), coinciding with leaf emergence and increased incoming radiation. A transition in energy partitioning was also observed after leaf fall, but the rate of change was greatly reduced. Wilson et al. (2001) observed this same trend for a broadleaf deciduous forest in Oak Ridge, TN, and attributed the more gradual fall transition to non-uniform timing of senescence, a warmer atmosphere, and negative soil heat fluxes.

Whole ecosystem LE was low during leaf-free periods, $<0.2$ MJ m$^{-2}$ day$^{-1}$, and was highly variable

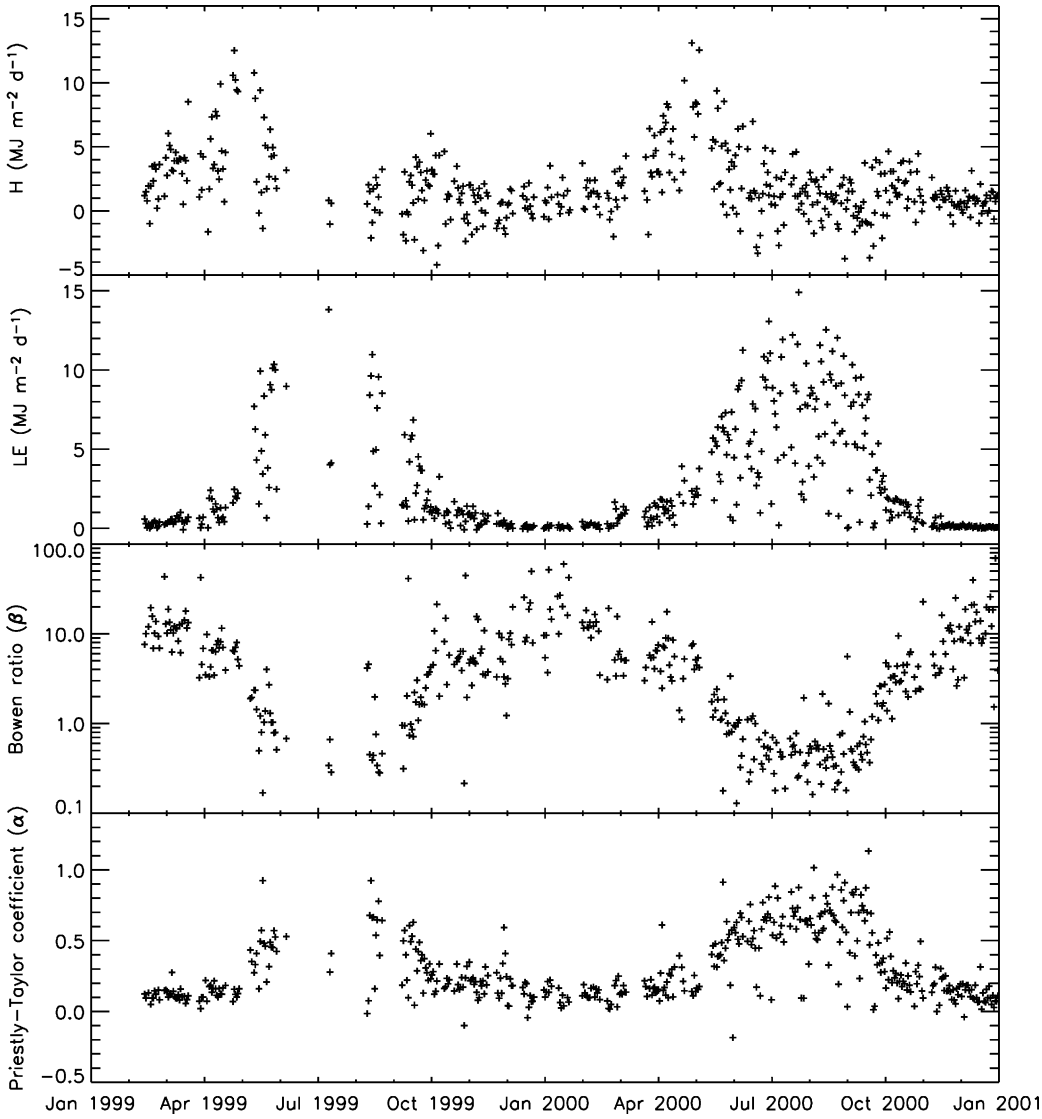


Fig. 13. Seasonal changes in daily integrated (a) sensible and (b) latent heat fluxes; (c) integrated midday (1000–1400 CST) Bowen ratio; (d) the Priestly–Taylor constant, $\alpha = ET_{Actual}/ET_{eq}$, from the Willow Creek flux tower (1999–2000).

during the growing season (Fig. 13). Day-to-day fluctuations were associated with daily energy inputs, and Bowen ratios ranged between about 0.3 and 0.6 during the growing season. This partitioning was comparable to a hardwood forest in Michigan of similar age and latitude, but slightly different species composition and soils (Schmid et al., 2003). During the growing season, ET approached that of a saturated surface, $ET_{actual}/ET_{eq} \approx 1$ (Fig. 13); where equilibrium evapotranspiration ($ET_{eq}$) is the evaporation rate derived from air temperature and available energy. Observed Priestly–Taylor coefficients ($\alpha = ET_{actual}/ET_{eq}$) were not sensitive to the amount of water in the upper 1 m of soil (Fig. 2), indicating that ET was controlled at the leaf level, and not by limitations imposed by soil water availability (e.g., Iacobelli and McCaughey, 1993). Daily averaged LE was more variable than have been observed at other locations (Anthoni et al.,

1999; Wilson et al., 2000), also suggesting that transpiration was not limited by high moisture tensions imposed by low soil hydraulic conductivity.

Whole-canopy fluxes of $CO_2$ and water vapor are closely linked in some forests (Baldocchi and Meyers, 1998), and show varying degrees of coupling with net radiation, vapor pressure deficit (VPD), and aerodynamic and canopy resistances (Verma et al., 1986). Using individual leaves, Lange et al. (1971) demonstrated that stomata respond directly to atmospheric humidity, and Wong et al. (1979) demonstrated that stomatal aperture could control carbon assimilation. Following the example of Anthoni et al. (1999), we compared the effect of VPD on the exchange of water vapor and $CO_2$ for specific levels of incoming radiation (Fig. 14). Incoming radiation influences surface leaf temperatures and VPD, and each has a distinctive affect on stomata opening and leaf conductance (Kutsch et al., 2001a; Lange et al., 1971). Priestly–Taylor coefficients ($\alpha$) responded positively to VPD (Fig. 14), and this response (i.e., slope) diminished with increased sunlight. Stomatal control over both transpiration and photosynthesis was evident only at VPD $>$ 1.5 kPa, and generalized dependencies of $\alpha$ and GEP on VPD were absent below this critical level (Fig. 14). Effects of stomotal closure on modeled estimates of NEE and GEP at Willow Creek were expected to be minimal, since half-hourly VPD seldom exceeded 1.5 kPa during the 1999 and 2000 growing seasons (Fig. 2).

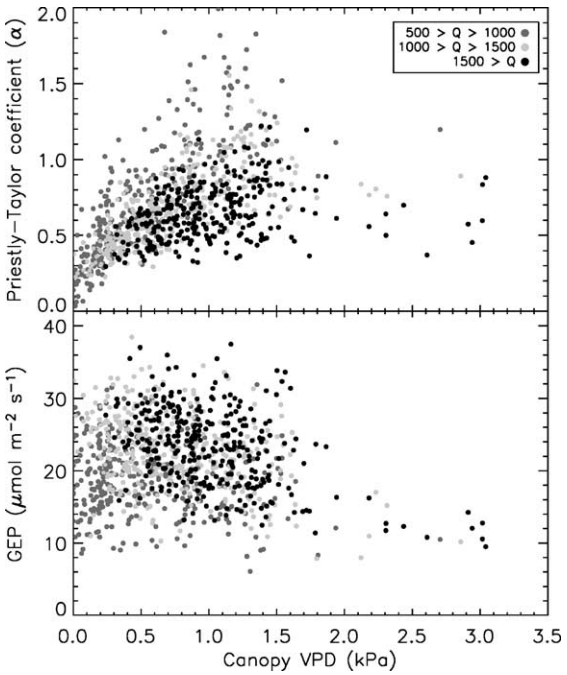


Fig. 14. Influence of half-hourly vapor pressure deficits (VPD) and incoming radiation on (a) relative evapotranspiration and (b) gross ecosystem production (GEP) observed from the Willow Creek flux tower during 2000. Symbol color indicates level of photosynthetically active radiation ($Q$): medium gray, 500–1000 μmol $m^{-2}$ $s^{-1}$; light gray, 1000–1500 μmol $m^{-2}$ $s^{-1}$; black, >1500 μmol $m^{-2}$ $s^{-1}$). Data was screened for precipitation events and condensation to avoid the confounding effects of water on leaves and sensors.

## 4. Conclusions

We observed seasonal patterns of carbon exchange and evaporation from an upland deciduous forest in north central Wisconsin during 1999 and 2000. The site is one of several observation points in the Great Lakes region that will be used to scale-up component and eddy covariance measurements from discrete ecosystems to landscape-scale observations from the WLEF tall tower near Park Falls, WI (Davis et al., 2003), and for regional model validation (Baker et al., 2003; Denning et al., 2003). We estimated that cumulative NEE of $CO_2$ at the Willow Creek site was $-334$ g C $m^{-2}$ $year^{-1}$ during the 2000 calendar year, which was greater than ecological inventory estimates of NEP (188 g C $m^{-2}$ $year^{-1}$) that spanned a long period of time. Annual rates of carbon accrual were quite large when compared with landscape-scale observations from the WLEF tall tower, and only slightly higher than other deciduous forests at this latitude. Partitioning of carbon between ER and GEP was 817 and 1165 g C $m^{-2}$, respectively. Surface energy imbalances and discrepancies between tower- and chamber-fluxes were similar to other sites, and ongoing studies have been initiated to address these concerns.

Gradient Richardson numbers above the forest canopy indicated decoupling of the sub-canopy on most nights throughout the growing season, and an analysis of expected ecosystem respiration (ER) during nighttime and daytime hours was used to ensure confidence in summed turbulent and storage fluxes above friction velocities ($u_*$) of 0.3 m $s^{-1}$. Screening of data below this turbulence threshold had

a relatively small effect of annual NEE (21 g C $m^{-2}$), suggesting that advection was not problematic at this site. However, we did encounter systematic errors associated with nighttime and early morning venting anomalies from a seemingly homogenous area to the SE of the tower. Circumstantial evidence for cold-air drainage of $CO_2$ has been presented at other sites, but this was the first documented case of apparent preferential venting of what might be pooled $CO_2$. Venting anomalies were characterized by unusually high turbulent flux measurements, some as high as 80 μmol $m^{-2}$ $s^{-1}$, that lasted for hours at a time without being compensated by changes in $CO_2$ storage. Times series, spectral analysis, $u_*$ values, and data from other flux towers in the area confirmed the validity of these observations. Comparisons of flux data from various wind directions revealed that fluxes from the SE quadrant were not representative of the local stand, and adding these measurements to our annual sums could not be justified. Consequently, all data from the SE quadrant (about 15% of the observations from all directions) was excluded from carbon exchange models and estimates of annual NEE.

Ecosystem respiration (ER) rates ranged from 0.1 to 6 μmol $m^{-2}$ $s^{-1}$, and half-life estimates at 25 °C ranged from 1 to 3 years. Measurements of carbon pools and annual cumulative ER were used to estimate an average carbon turnover time of 22 years. Thermodynamic parameters used to model ER suggested that quantity and quality of litter fall, not just temperature, seemed to have a measurable influence on ER throughout the year. Daily integrated rates of gross ecosystem production (GEP) were greater than most deciduous forests, about 13 g C $m^{-2}$ day, which is a characteristic of higher latitude forests with relatively short growing seasons. Photosynthetic uptake rates were affected by phenological stage, sun angle, chlorophyll and anthocyanin content, light quantity and quality, and vapor pressure deficits (VPD).

Surface soil moisture contents were high throughout 1999 and 2000, ranging from 0.26 to 0.40 $m^3$ $m^{-3}$, and variation in the water content of the upper 1 m of soil had no discernable influence on rates of evapotranspiration (ET) during the growing season. Latent heat fluxes were depressed (<0.2 MJ $m^{-2}$ $day^{-1}$) during the leaf-off period, and increased dramatically from June through September due to forest transpiration. Forest transpiration allowed ET to approach levels approximating a saturated surface ($ET_{eq}$), and partial closure of stomata influenced Priestly–Taylor coefficients ($\alpha$) at all light intensities. In contrast, total exchange of $CO_2$ was only affected under intense sunlight ($Q >$ 1500 μmol $m^{-2}$ $s^{-1}$) and high vapor pressure deficits (VPD $>$ 1.5 kPa). Quantifying these physiological relationships will help us develop more realistic empirical models for predicting carbon and water vapor fluxes from observations of incoming radiation, leaf temperature, and humidity.

## Acknowledgements

This research was funded in part by the National Institute for Global Environmental Change through the US Department of Energy (DoE). Any opinions, findings, and conclusions or recommendations herein are those of the authors and do not necessarily reflect the view of DoE. The Atmospheric Chemistry Project of the Climate and Global Change Program of the National Oceanic and Atmospheric Administration supported P. Bakwin. The authors wish to thank Art Johnston, Aaron Berger, Dan Baumann, and all those who contributed to the construction and maintenance of this flux tower. We also extend our appreciation to Dana Carrington for data analysis, and to Tom Steele, Gary Kellner, and Karla Ortman at the Kemp Natural Resources Station, University of Wisconsin, who provided technical support and accommodations throughout this project.

## References

Anthoni, P.M., Law, B.E., Unsworth, M.H., 1999. Carbon and water vapor exchange of an open-canopied ponderosa pine ecosystem. Agric. For. Meteorol. 95, 151–168.

Aubinet, M., Grelle, A., Ibrom, A., Rannik, Ü., Moncrieff, J., Foken, T., Kowalski, A.S., Martin, P.H., Berbigier, P., Bernhofer, C., Clement, R., Elbers, J., Granier, A., Grünwald, T., Morgenstern, K., Pilegaard, K., Rebmann, C., Snijders, W., Valentini, R., Vesala, T., 2000. Estimates of the annual net carbon and water exchange in European forests: The EUROFLUX methodology. Adv. Ecol. Res. 30, 114–175.

Baker, I., Denning, A.S., Hanan, N., Prihodko, L., Uliasz, M., Vidale, P-L., Davis, K., Bakwin, P., 2003. Simulated and observed fluxes of sensible and latent heat and $CO_2$ at the WLEF-TV tower using SiB2.5. Glob. Change Biol. 9, 1262–1277.

Bakwin, P.S., Tans, P.P., Zhao, C.L., Ussler, W., Quesnell, E., 1995. Measurements of carbon dioxide on a very tall tower. Tellus B 47, 535–549.

Bakwin, P.S., Tans, P.P., Hurst, D.F., Zhao, C., 1998. Measurements of carbon dioxide on very tall towers: results of the NOAA/CMDL program. Tellus, Ser. B 50, 401–415.

Baldocchi, D., Flage, E., Gu, L., Olson, R., Hollinger, D., Running, S., Athoni, P., Bernhoffer, C., Davis, K., Evans, B., Fuentes, J., Goldstein, A., Katul, G., Law, B., Lee, X., Malhi, Y., Meyers, T., Munger, W., Oechel, W., Paw, U.K.T., Pilegaard, K., Schmid, H.P., Valentini, R., Verma, S., Vesala, T., Wilson, K., Wofsy, S., 2001. FLUXNET: a new tool to study the temporal and spatial variability of ecosystem-scale carbon dioxide, water vapor, and energy flux densities. Bull. Am. Meteorol. Soc. 82, 2415–2434.

Baldocchi, D., Meyers, T., 1998. On using eco-physiological, micrometeorological and biogeochemical theory to evaluate carbon dioxide, water vapor, and trace gas fluxes over vegetation: a perspective. Agric. For. Meteorol. 90, 1–25.

Baldocchi, D.D., Meyers, T.P., 1991. Trace gas exchange above the floor of a deciduous forest. 1. Evaporation and $CO_2$ efflux. J. Geophys. Res. 96, 7271–7285.

Barford, C.C., Wofsy, S.C., Goulden, M.L., Munger, J.W., Pyle, E.H., Urbanski, S.P., Hutyra, L., Saleska, S.R., Fitzjarrald, D., Moore, D., 2001. Factors controlling long- and short-term sequestration of atmospheric $CO_2$ in a mid-latitude forest. Science 294, 1688–1691.

Berger, B.W., Davis, K.J., Yi, C., Bakwin, P.S., Zhao, C.L., 2001. Long-term carbon dioxide fluxes from a very tall tower in a northern forest: flux measurement methodology. J. Atmos. Ocean. Technol. 18, 529–542.

Bergh, J., Linder, S., 1999. Effects of soil warming during spring on photosynthetic recovery in boreal Norway spruce stands. Glob. Change Biol. 5, 245–253.

Bird, R.E., Hulstrom, R.L., 1981. A simplified clear sky model for direct and diffuse insolation on horizontal surfaces. SERI Technical Report SERI/TR-642-761. Solar Energy Research Institute, Golden, CO.

Bolstad, P.V., Davis, K.J., Martin, J., Cook, B.D., Wang, W., 2004. Component and whole-system respiration fluxes in northern deciduous forests. Tree Physiol. 24, 493–504.

Brooks, P.D., Schmidt, S.K., Williams, M.W., 1997. Winter production of $CO_2$ and $N_2O$ from alpine tundra: environmental controls and relationship to inter-system C and N fluxes. Oecologia 110, 403–413.

Caspersen, J.P., Pacala, S.W., Jenkins, J.C., Hurtt, G.C., Moorcroft, P.R., Birdsey, R.A., 2000. Contributions of land-use history to carbon accumulation in US forests. Science 290, 1148–1151.

Ciais, P., Tanss, P.P., Trolier, M., White, J.W.C., Francey, R.J., 1995. A Large northern hemisphere terrestrial $CO_2$ sink indicated by the $^{13}C/^{12}C$ ratio of atmospheric $CO_2$. Science 269, 1098–1102.

Clark, D.A., Brown, S., Kicklighter, D.W., Chambers, J.Q., Thomlinson, J.R., Ni, J., 2001. Measuring net primary production in forests: concepts and field methods. Ecol. Appl. 11, 356–370.

Cole, K.L., Davis, M.B., Stearns, F., Guntenspergen, G., Walker, K., 1999. Historical landcover changes in the Great Lakes Region. In: Sisk, T.D. (Ed.), Perspectives on the Land-use History of North America: A Context for Understanding Our Changing Environment, Chapter 6. US Geological Survey, Biological Resources Division, Biological Science Report USGS/BRD/BSR 1998-0003 (revised September 1999).

Conway, T.J., Tans, P.P., Waterman, L.S., Thoning, K.W., Kitzis, D.R., Masarie, K.A., Zhang, N., 1994. Evidence for interannual variability of the carbon cycle from the National Oceanic and Atmospheric Administration/Climate Monitoring and Diagnostics Laboratory Global Air Sampling Network. J. Geophys. Res. 99, 22831–22855.

Cook, B.D., Davis, K.J., Wang, W., Bakwin, P.S., Yi, C., Bolstad, P.V., Isebrands, J.G., Teclaw, R.M., 2001. Contributions from a deciduous forest and shrub wetland to regional carbon fluxes in northern Wisconsin. Eos. Trans. AGU 82(47), Fall Meeting Supplement, Abstract B42A-0114.

Cornish-Bowden, A., 2002. Enthalpy–entropy compensation: a phantom phenomenon. J. Biosci. 27, 121–126.

Curtis, J.T., 1959. The Vegetation of Wisconsin. University of Wisconsin Press, Madison, 657 pp.

Curtis, P.S., Hanson, P.J., Bolstad, P., Barford, C., Randolph, J.C., Schmid, H.P., Wilson, K.B., 2002. Biometric and eddy-covariance based estimates of annual carbon storage in five eastern North American deciduous forests. Agric. For. Meteorol. 113, 3–19.

Davis, K.J., Bakwin, P.S., Yi, C., Berger, B.W., Zhao, C., Teclaw, R.M., Isebrands, J.G., 2003. The annual cycles of $CO_2$ and $H_2O$ exchange over a northern mixed forest as observed from a very tall tower. Glob. Change Biol. 9, 1278–1293.

Denning, S.A., Nicholls, M., Prihodko, L., Baker, I., Vidale, P-L., Davis, K., Bakwin, P., 2003. Simulated variations in atmospheric $CO_2$ over a Wisconsin forest using a coupled ecosystem–atmosphere model. Glob. Change Biol. 9, 1241–1250.

Dore, S., Hymus, G.J., Johnson, D.P., Hinkle, C.R., Valentini, R., Drake, B.G., 2003. Cross validation of open-top chamber and eddy covariance measurements of ecosystem $CO_2$ exchange in a Florida scrub–oak ecosystem. Glob. Change Biol. 9, 84–95.

Ehman, J.L., Schmid, H.P., Grimmond, C.S.B., Randolph, J.C., Hanson, P.J., Wayson, C.A., Cropley, F.D., 2002. An initial intercomparison of micrometeorological and ecological inventory estimates of carbon exchange in a mid-latitude deciduous forest. Glob. Change Biol. 8, 575–589.

Eyring, H.J., 1935. The activated complex in chemical reactions. J. Chem. Phys. 3, 107–115.

Falge, E., Baldocchi, D., Tenhunen, J., Aubinet, M., Bakwin, P., Berbigier, P., Bernhofer, C., Burba, G., Clement, R., Davis, K.J., Elbers, J.A., Goldstein, A.H., Grelle, A., Granier, A., Guðmundsson, J., Hollinger, D., Kowalski, A.S., Katul, G., Law, B.E., Malhi, Y., Meyers, T., Monson, R.K., Munger, J.W., Oechel, W., Paw, U.K.T., Pilegaard, K., Rannik, Ü., Rebmann, C., Suyker, A., Valentini, R., Wilson, K., Wofsy, S., 2002. Seasonality of ecosystem respiration and gross primary production as derived from FLUXNET measurements. Agric. For. Meteorol. 113, 53–74.

Falge, E., Baldocchi, D., Olson, R., Anthoni, P., Aubinet, M., Bernhofer, C., Burba, G., Ceulemans, R., Clement, R., Dolman, H., Granier, A., Gross, P., Grünwald, T., Hollinger, D., Jensen, N.O., Katul, G., Keronen, P., Kowalski, A., Lai, C.T., Law, B.E., Meyers, T., Moncrieff, J., Moors, E., Munger, J.W., Pilegaard,

K., Rannik, Ü., Rebmann, C., Suyker, A., Tenhunen, J., Tu, K., Verma, S., Vesala, T., Wilson, K., Wofsy, S., 2001. Gap filling strategies for defensible annual sums of net ecosystem exchange. Agric. For. Meteorol. 197, 43–69.

Fang, C., Moncrieff, J.B., 2001. The dependence of soil $CO_2$ efflux on temperature. Soil Biol. Biochem. 33, 155–165.

Goulden, M.L., Munger, J.W., Fan, S.M., Daube, B.C., Wofsy, S.C., 1996a. Exchange of carbon dioxide by a deciduous forest: response to interannual climate variability. Science 271, 1576–1578.

Goulden, M.L., Munger, J.W., Fan, S-M., Daube, B.C., Wofsy, S.C., 1996b. Measurements of carbon sequestration by long-term eddy-covariance: methods and a critical evaluation of accuracy. Glob. Change Biol. 2, 169–182.

Gower, S.T., Krankine, O., Olson, R.J., Apps, M., Linder, S., Wang, C., 2001. Net primary production and carbon allocation patterns of boreal forest ecosystems. Ecol. Appl. 11, 1395–1411.

Gu, L., Fuentes, J.D., Shugart, H.H., Staebler, R.M., Black, T.A., 1999. Response of net ecosystem exchanges of carbon dioxide to changes in cloudiness: results from two North American deciduous forests. J. Geophys. Res. 104 (D24), 31421–31434.

Gunderson, C.A., Norby, R.J., Wullschleger, S.D., 2000. Acclimation of photosynthesis and respiration to simulated climatic warming in northern and southern populations of *Acer saccharum*: laboratory and field evidence. Tree Physiol. 20, 87–96.

Hanson, P.J., Edwards, N.T., Garten, C.T., Andrews, J.A., 2000. Separating root and soil microbial contributions to soil respiration: a review of methods and observations. Biogeochemistry 48, 115–146.

Högberg, P., Nordgren, A., Buchmann, N., Taylor, A.F.S., Ekblad, A., Högberg, M.N., Nyberg, G., Ottosson-Löfvenius, M., Read, D.J., 2001. Large-scale forest girdling shows that current photosynthesis drives soil respiration. Nature 411, 789–792.

Hole, F.D., 1976. Soils of Wisconsin. University of Wisconsin Press, Madison.

Horst, T.W., Weil, T.W., 1994. How far is far enough? The Fetch requirements for micrometeorological measurement of surface fluxes. J. Atmos. Ocean. Technol. 11, 1018–1025.

House, J.I., Prentice, I.C., Ramankutty, N., Houghton, R.A., Heimann, M., 2003. Reconciling apparent inconsistencies in estimates of terrestrial $CO_2$ sources and sinks. Tellus B 55, 345–363.

Houghton, R.A., 2003. Why are estimates of the terrestrial carbon balance so different? Glob. Change Biol. 9, 500–509.

Houghton, J.T., Ding, Y., Griggs, D.J., Noguer, M., van der Linden, P.J., Xiaosu, D. (Eds.), 2001. Climate Change 2001: The Scientific Basis. Cambridge University Press, Cambridge, 896 pp.

Iacobelli, A., McCaughey, J.H., 1993. Stomatal conductance in a northern temperate deciduous forest: temporal and spatial patterns. Can. J. For. Res. 23, 245–252.

Irvine, M.R., Gardiner, B.A., Hill, M.K., 1997. The evolution of turbulence across a forest edge. Boundary-Layer Meteorol. 84, 467–496.

Keeling, R.F., Piper, S.C., Heimann, M., 1996. Global and hemispheric $CO_2$ sinks deduced from changes in atmospheric $O_2$ concentration. Nature 381, 218–221.

Kitzis, D., Zhao, C.L., 1999. CMDL/carbon cycle greenhouse gases group standards preparation and stability. National Oceanic and Atmospheric Administration Technical Memorandum ERL-14. Climate Monitoring and Diagnostics Laboratory, Boulder, CO, 14 pp.

Krug, R.R., Hunter, W.G., Grieger, R.A., 1976. Enthalpy–entropy compensation. I. Some fundamental statistical problems associated with the analysis of van't Hoff and Arrhenius data. J. Phys. Chem. 80, 2335–2341.

Kutsch, W.L., Herbst, M., Vanselow, R., Hummelshøj, P., Jensen, N.O., Kappen, L., 2001a. Stomatal acclimation influences water and carbon fluxes of a beech canopy in northern Germany. Basic Appl. Ecol. 2, 265–281.

Kutsch, W.L., Staack, A., Wötzel, J., Middelhoff, U., Kappen, L., 2001b. Field measurements of root respiration and total soil respiration in an alder forest. New Phytol. 150, 157–168.

Lafleur, P.M., McCaughey, J.H., Joiner, D.W., Bartlett, P.A., Jelinski, D.E., 1997. Seasonal trends in energy, water, and carbon dioxide fluxes in a northern boreal wetland. J. Geophys. Res. 102, 29009–29020.

Lange, O.L., Lösch, R., Schulze, E.D., Kappen, L., 1971. Responses of stomata to changes in humidity. Planta 100, 76–86.

Larigauderie, A., Körner, C., 1995. Acclimation of leaf dark respiration to temperature in alpine and lowland plant species. Ann. Bot. 76, 245–252.

LaVigne, M.B., Ryan, M.G., Anderson, D.E., Baldocchi, D.D., Crill, P.M., Fitzjarald, D.R., Goulden, M.L., Gower, S.T., Massheder, J.M., McCaughey, J.H., Rayment, M., Striegl, R.G., 1997. Comparing nocturnal eddy covariance measurements to estimates of ecosystem respiration made by scaling chamber measurements at six coniferous boreal sites. J. Geophys. Res. 102, 28977–28985.

Law, B.E., Falge, E., Gu, L., Baldocchi, D.D., Bakwin, P., Berbigier, P., Davis, K., Dolman, A.J., Falk, M., Fuentes, J.D., Goldstein, A., Granier, A., Grelle, A., Hollinger, D., Janssens, I.A., Jarvis, P., Jensen, N.O., Katul, G., Mahli, Y., Matteucci, G., Meyers, T., Monson, R., Munger, W., Oechel, W., Olson, R., Pilegaard, K., Paw, U.K.T., Thorgeirsson, H., Valentini, R., Verma, S., Vesala, T., Wilson, K., Wofsy, S., 2002. Environmental controls over carbon dioxide and water vapor exchange of terrestrial vegetation. Agric. For. Meteorol. 113, 97–120.

Law, B., Ryan, M.G., Anthoni, P., 1999. Seasonal and annual respiration of a ponderosa pine ecosystem. Glob. Change Biol. 5, 169–182.

Lee, X., Fuentes, J.D., Staebler, R.M., Neumann, H.H., 1999. Long-term observation of the atmospheric exchange of $CO_2$ with a temperate deciduous forest in southern Ontario, Canada. J. Geophys. Res. 104, 15975–15984.

Li-Cor, Incorporated, 1996. LI-6262 $CO_2/H_2O$ Analyzer Operating and Service Manual. Publication 9003-59. Li-Cor, Environmental Division, Lincoln, NE, 100 pp.

Lloyd, J., Taylor, J.A., 1994. On the temperature dependence of soil respiration. Funct. Ecol. 8, 315–323.

Luo, Y., White, L.W., Canadell, J.G., DeLucia, E.H., 2003. Sustainability of terrestrial carbon sequestration: a case study in Duke Forest with inversion approach. Glob. Biogeochem. Cycl. 17, 1021. doi: 10.1029/2002GB001923.

Mahrt, L., Lee, X., Black, A., Neumann, H., Staebler, R.M., 2000. Nocturnal mixing in a forest subcanopy. Agric. For. Meteorol. 101, 67–78.

Mahrt, L., 1998. Flux sampling errors for aircraft and towers. J. Atmos. Ocean. Technol. 15, 416–429.

Mahrt, L., 1985. Vertical structure and turbulence in the very stable boundary layer. J. Atmos. Sci. 42, 2333–2349.

Massman, W.J., 1987. A comparative study of some mathematical models of mean wind structure and aerodynamic drag of plant canopies. Boundary Layer Meteorol. 40, 179–197.

Moncrieff, J., Valentini, R., Greco, S., Seufert, G., Ciccioli, P., 1997. Trace gas exchange over terrestrial ecosystems: methods and perspectives in micrometeorology. J. Exp. Bot. 48, 1133–1142.

Pacala, S.W., Hurtt, G.C., Baker, D., Peylin, P., Houghton, R.A., Birdsey, R.A., Heath, L., Sundquist, E.T., Stallar, R.F., Ciais, P., Moorcroft, P., Caspersen, J.P., Shevliakova, E., Moore, B., Kohlmaier, G., Holland, E., Gloor, M., Harmon, M.E., Fan, S.M., Sarmiento, J.L., Goodale, C.L., Schimel, D., Field, C.B., 2001. Consistent land- and atmosphere-based US carbon sink estimates. Science 292, 2316–2320.

Pattey, E., Desjardins, R.L., St-Amour, G., 1997. Mass and energy exchanges at a southern old black spruce site during key periods of BOREAS. J. Geophys. Res. D 102, 28967–28976.

Post, W.M., Kwon, K.C., 2000. Soil carbon sequestration and land-use change: processes and potential. Glob. Change Biol. 6, 317–327.

Press, W.H., Teukolsky, S.A., Vetterling, W.T., Flannery, B.P., 1992. Numerical Recipes in C: The Art of Scientific Programming, 2nd ed. Cambridge University Press, .

Research Systems Incorporated, 1998. Interactive Data Language Reference Guide, Version 5.1 Edition. Research Systems Incorporated, Boulder, CO.

Ruimy, A., Jarvis, P.G., Baldocchi, D.D., Saugier, B., 1995. $CO_2$ fluxes over plant canopies and solar radiation: a review. Adv. Ecol. Res. 26, 1–51.

Russell, C.A., Veroney, R.P., 1998. Carbon dioxide efflux from the floor of a boreal aspen forest: relationship to environmental variables and estimates of C respired. Can. J. Soil Sci. 78, 301–310.

Ryan, M.G., Lavigne, M.B., Gower, S.T., 1997. Annual carbon cost of autotrophic respiration in boreal forest ecosystems in relation to species and climate. J. Geophys. Res. 102, 28871–28883.

Savage, K.E., Davidson, E.A., 2001. Interannual variation of soil respiration in two New England forests. Glob. Biogeochem. Cycl. 15, 337–350.

Schlesinger, W.H., 1997. San Diego, CA, Biogeochemistry: an analysis of global change, 2nd ed. Academic Press, 592 pp.

Schmid, H.P., Su, H.-B., Vogel, C.S., Curtis, P.S., 2003. Ecosystem–atmosphere exchange of carbon dioxide over a mixed hardwood forest in northern lower Michigan. J. Geophys. Res. 108 (D14), 4417. doi: 10.1029/2002JD003011.

Schmid, H.P., Grimmond, S.B., Cropley, F., Offerle, B., Su, H.B., 2000. Measurements of $CO_2$ and energy fluxes in the mid-western United States. Agric. For. Meteorol. 103, 357–374.

Schulte, L.A., Mladenoff, D.J., 2001. The original US public land survey records: their use and limitations in reconstructing pre-settlement vegetation. J. For. 99 (10), 5–10.

Silvola, J., Alm, J., Ahlholm, U., Nykänen, H., Martikainen, P.J., 1996. $CO_2$ fluxes from peat in boreal mines under varying temperature and moisture conditions. J. Ecol. 84, 219–228.

Tans, P.P., Fung, I.Y., Takahashi, T., 1990. Observational constraints on the global atmospheric $CO_2$ budget. Science 247, 1431–1438.

Ter-Mikaelian, M.T., Korzukhin, M.D., 1997. Biomass equations for sixty-five North American tree species. For. Ecol. Manage. 97, 1–24.

Tjoelker, M.G., Oleksyn, J., Reich, P.B., 2001. Modeling respiration of vegetation: evidence for a general temperature-dependent $Q_{10}$. Glob. Change Biol. 7, 223–230.

Twine, T.E., Kustas, W.P., Norman, J.M., Cook, D.R., Houser, P.R., Meyers, T.P., Prueger, J.H., Starks, P.J., Wesely, M.L., 2000. Correcting eddy-covariance flux underestimates over grassland. Agric. For. Meteorol. 103, 279–300.

Updegraff, K., Pastor, J., Bridgham, S.D., Johnston, C.A., 1995. Environmental and substrate controls over carbon and nitrogen mineralization in northern wetlands. Ecol. Appl. 5, 151–163.

Verma, S.B., Kim, J., Clement, R.J., Shurpali, N.J., Billesbach, D.P., 1995. Trace gas and energy fluxes: micrometeorological perspectives. In: Lal, R., Kimble, J., Levine, E., Stewart, B.A. (Eds.), Soils and Global Change. Lewis Publishers, Boca Raton, FL, pp. 361–376.

Verma, S.B., Baldocchi, D.D., Anderson, D.E., Matt, D.R., Clement, R.J., 1986. Eddy fluxes of $CO_2$, water vapor, and sensible heat over a deciduous forest. Boundary-Layer Meteorol. 36, 71–91.

Walters, M.B., Reich, P.B., 1997. Growth of *Acer saccharum* seedlings in deeply shaded understories of northern Wisconsin: effects of nitrogen and water availability. Can. J. For. Resour. 27, 237–247.

Wilson, K.B., Goldstein, A., Falge, E., Aubinet, M., Baldocchi, D., Berbigier, P., Bernhofer, C., Ceulemans, R., Dolman, H., Field, C., Grelle, A., Ibrom, A., Law, B.E., Kowalski, A., Meyers, T., Moncrieff, J., Monson, R., Oechel, W., Tenhunen, J., Valentini, R., Verma, S., 2002. Energy balance closure at FLUXNET sites. Agric. For. Meteorol. 113, 223–243.

Wilson, K.B., Baldocchi, D., Hanson, P.J., 2001. Leaf age affects the seasonal pattern of photosynthetic capacity and net ecosystem exchange of carbon in a deciduous forest. Plant Cell Environ. 24, 571–583.

Wilson, K.B., Hanson, P.J., Baldocchi, D.D., 2000. Factors controlling evaporation and energy partitioning beneath a deciduous forest over an annual cycle. Agric. For. Meteorol. 102, 83–103.

Wong, S.C., Cowan, I.R., Farquhar, G.D., 1979. Stomatal conductance correlates with photosynthetic capacity. Nature 282, 424–426.

Yi, C., Davis, K.J., Bakwin, P.S., Berger, B.W., Marr, L.C., 2000. Influence of advection on the measurements of the net ecosystem–atmosphere exchange of $CO_2$ from a very tall tower. J. Geophys. Res. 105 (D8), 9991–9999.

Zhao, C.L., Bakwin, P.S., Tans, P.P., 1997. A design for unattended monitoring of carbon dioxide on a very tall tower. J. Atmos. Ocean. Technol. 14, 1139–1145.

Zogg, G.P., Zak, D.R., Burton, A.J., Pregitzer, K.S., 1996. Fine root respiration in northern hardwood forests in relation to temperature and nitrogen availability. Tree Physiol. 16, 719–725.